Proposing an Improved Surface Dryness Index to Estimate Soil Moisture Based on the Temperature Vegetation Dryness Index

by

Lei Luo

B.S., China University of Geosciences (Beijing), 2014

A THESIS

submitted in partial fulfillment of the requirements for the degree

MASTER OF ARTS

Department of Geography
College of Arts and Sciences

KANSAS STATE UNIVERSITY
Manhattan, Kansas

2017

Approved by:

Major Professor
Douglas Goodin

Copyright

© Lei Luo 2017

Abstract

In this thesis, I proposed a new surface dryness index based on the slope of soil moisture isolines in the Land Surface Temperature/Normalized Difference Vegetation Index (LST/NDVI) feature space. This index, referred to here as Dryness Slope Index (DSI), overcomes the problem of Temperature Vegetation Dryness Index (TVDI) having different basis when calculating TVDI values across different images. This problem is rooted in the definition of TVDI whose calculation depends on the position of the "dry edge" and "wet edge" of pixels' values in the LST/NDVI space of a specific image. The "wet edge" has a fairly stable physical meaning, which represents soil at field capacity or above, and it remains stable across a time series of images. However, the position of "dry edge" represents the driest condition in the image, which does not necessarily mean that the soil is completely dry. Therefore, the value of TVDI calculated from different images is not based on an invariant dry edge value as its baseline, and it is therefore likely to lead to incorrect conclusion if used without extra examination. This problem manifests itself when comparing TVDI values from different images with meteorological data. Results from similar analyses done with DSI showed more reasonable match with the validation data, indicating DSI is a more robust surface dryness index than TVDI.

Having verified DSI can be effectively used in estimating soil moisture, I applied DSI on Landsat5 TM to study the relationship between soil moisture and land cover, slope, aspect, and relative elevation. Results showed that land cover accounts the most for variations of estimated soil moisture. I also applied DSI on a long time-series (2000 to 2014) of MODIS data trying to explore the temporal evolution of soil moisture in the entire Flint Hills ecoregion. Results showed little correlation between time and estimated soil moisture, indicating that no noticeable changes in soil moisture has been found through all these years.

Table of Contents

List of Figures

List of Tables

Acknowledgements

The completion of this thesis would not have been possible without the support from many people. First of all, I am enormously thankful for my academic advisor Dr. Douglas G. Goodin who has always given me guidance to find the nearest path to problems as well as challenges to make myself achieve more than I could. You have supported me academically, financially, and mentally which has made one of my hardest journey so enjoyable and rewarding. You were always there when I needed help, academic or not, and you were so patient to help resolve my concerns and so supportive about my decisions. To my committee members, Dr. Jida Wang and Dr. J.M. Shawn Hutchinson, your numerous perspectives and approaches have given me tremendous help in completing this thesis. To Dr. Robert B. McKane and other researchers from the U.S. Environmental Protection Agency, Western Ecology Division, thank you for spending numerous time over the phone to give me insights on the subject as well as data I needed for completing this thesis.

To all the people I have met at K-State, particularly graduate students within the Department of Geography, your kindness and help have made my transition as an international student much easier and enjoyable than I could have ever imagined. To two of my best friends Lianling Su and Thomas Larsen, you have showed me so many interesting things and provided me tremendous help, and your optimism has always encouraged me to march forward with great joy. To my family, your support throughout my academic career has been extraordinary. Thanks to all your efforts and relentless support, I have come so far academically and in life. Thank you for bearing burdens with me and always believing in me even when I had doubts about myself.

To the Department of Geography and K-State, thank you for making this great journey possible and showing me how to find myself and how I can make a difference in the world.

Chapter 1 – Introduction

Soil moisture is widely recognized as an important variable in environmental studies related to meteorology and agriculture (Ahmad & Bastiaanssen, 2003; Vischel *et al.*, 2008; Mattia *et al*., 2009; Kong *et al.*, 2011). It is also a key hydrologic parameter linked to water availability, land surface evapotranspiration, runoff generation, groundwater recharge, and irrigation scheduling among other processes (Scott *et al.*, 2003). For hydrologic and agricultural purposes, the estimation of soil moisture is crucial as it controls the quantity of water available for vegetation growth (Cook *et al*., 2006), deep aquifer recharge (Seneriviratne *et al*., 2006; Kjellström *et al.*, 2007; Lam *et al*., 2011); and soil saturation, which controls the partitioning of rainfall between runoff and infiltration, and sediment transport (Vivoni *et al*., 2007; Ávila *et al.*, 2011). Knowledge of the spatial patterns of soil moisture is of immense importance to understand how much water is captured and in stored uplands, runoff available to downstream users, and recharge of groundwater. Flood prediction, including information on the spatial extent of inundation, discharge, and timing of the flood peak, and duration of recession, is critically dependent on soil moisture data. Similarly, changes in soil moisture at the land–atmosphere boundary are of critical importance to the parametrization of weather prediction and climate models (Scott *et al*., 2003; Oki *et al.* 1999; Walker and Houser 2001). Although the need for retrieving soil water content information at different scales is widely recognized, the high spatial and temporal variability of soil moisture caused by the heterogeneity of soil texture, topography, vegetation, and climate in the natural environment makes soil moisture difficult to measure (Bezerra *et al*., 2012b; Kong *et al*., 2011).

Generally speaking, soil water content can be obtained from three methods: (1) field measurements; (2) meteorological data; and (3) remote sensing. Field measurement provides the most accurate information on soil moisture condition. However, it is often done by installing permanent soil moisture probes into the soil at particular place, therefore it is costly and time-consuming especially for remote areas or areas across different countries. Developing countries are also likely to lack the necessary facilities for long-term monitoring of soil moisture. What is more, the spatial distribution of soil moisture based on interpolation of point-based data has limited frequency and spatial coverage of field investigations. Point-based data are also often poorly distributed and are insufficient and are often not available for timely water stress detection.

Technological advances in satellite remote sensing have offered an alternative to studying soil moisture and enabled us to monitor it at higher temporal and spatial resolutions at lower cost and time. Remote sensing covers a wide range of the electromagnetic spectrum, including the microwave, optical, and thermal regions, which can be utilized to estimate soil moisture. The theoretical basis for microwave remote sensing of soil moisture is that soil's dielectric properties heavily depends on its moisture condition. There is great distinction between wet soil and dry soil in terms of their dielectric constant, therefore soil moisture is manifested through the dielectric properties. Microwave techniques are capable of penetrating clouds, which makes it desirable at higher latitudes and in humid regions where cloud frequently covers the sky. Soil moisture can be estimated using airborne passive radiometers for soil depths between 0 and 10 centimeters (Schmugge 1999). However, one of the most noticeable limitations should be noted, which is that the spaceborne microwave remote sensing has a resolution varying between 50 to 150 kilometers (Scott *et al.,* 2003). Even though airborne passive radiometers are able to provide soil water information at higher spatial resolution, frequent flights are infeasible and often unaffordable. There are several active microwave sensors in the form of radars aboard on the RadarSat, EnviSat, the European remote sensing (ERS) satellite, Japan Earth resources (JERS) satellite, which provide observations at 20 ~ 30 meter spatial resolution. The Soil Moisture Active Passive (SMAP) was launched 31 January 2015 by NASA. It can provide measurements of the land surface soil moisture and freeze-thaw state with near-global revisit coverage in 2 ~ 3 days. It carries a radiometer that records microwave emissions from the top 5 cm in the soil with a spatial resolution of about 40 km, and radar will provide backscatter measurements at 1 km resolution. However, the ERS, JERS, and the radar of SMAP are no longer operational. What is more, active microwave sensors have limited ability to penetrate the vegetation layer and the backscatter coefficient is significantly affected by surface roughness (Ulaby and Elachi 1990; Verhoest *et al.* 1998; Hoeben and Troch 2000).

Optical/thermal remote sensing has attracted more attention and gained popularity in estimating soil moisture. In the visible and near-infrared wavelengths, the emission and reflection characteristics of a natural surface largely depend on the spectral response of vegetation and soil. The soil moisture status influences chlorophyll content in the leaves and in turn changes the spectral response of vegetation. Similarly, soil water content also affects the spectral response of soil as it is known that soil reflectance decreases with increasing soil water content. In middle

infrared region, soil with more water content shows lower reflectance. In the thermal infrared wavelengths, land objects vary in terms of temperature and emissivity which is largely controlled by their thermal inertia that represents the ability of a material to conduct and store heat. Soil moisture therefore can also influence the temperature of vegetation and surface soil. Water content changes in leaves because of the change of soil moisture can be detected in terms of variations of vegetation indices such as Normalized Difference Vegetation Index (NDVI). However, NDVI is a rather conservative indicator of water stress as vegetation remains green after initial water stress. However, LST can rise rapidly with water content decreasing. Therefore, land surface temperature and vegetation indices in combination can provide more comprehensive information on water content at the surface.

In the 1990s, the triangle method, a new approach to mapping both land surface moisture and surface turbulent energy fluxes gained popularity (Price, 1990, Carlson *et al*., 1994). This method allows the pixel distribution from the image to fix the boundary conditions for the model, thereby largely bypassing the need for ancillary atmospheric and surface data. The triangle method is based on an interpretation of the pixel distribution in the LST/NDVI feature space. LST is affected by many factors such as surface thermal properties, net radiation, evapotranspiration, and vegetation coverage, hence there is no direct relationship between LST and soil water content. However, soil moisture is an important factor controlling vegetation canopy temperature and under certain vegetation coverages soil moisture can indirectly affect canopy temperature. The calculation of the Temperature Vegetation Dryness Index (TVDI) is the based on the upper and lower boundaries on the LST/NDVI feature space (See Figure 1.1). The upper boundary, which is called the “dry edge”, represents the driest condition in the frame and the lower boundary referred here as the “wet edge” which represents the soil is at field capacity or above.

Research Questions and Structure of the Thesis

Even though the triangle method and TVDI have been widely used to estimate surface dryness condition, few studies have been carried out on the theoretical basis of the "triangle" method, and the use of TVDI without extra attention may lead to incorrect conclusions especially when comparing the dryness condition of several different dates by comparing their respective TVDI values. This is owing to by how TVDI is defined. TVDI is based on the position of the dry edge and that of the wet edge. The former, represents the driest condition in the frame, does not necessarily means that soil moisture is zero and is likely to vary for images from different days, whereas the latter has a fairly stable physical meaning, which is at field capacity or above. So, the calculation of TVDI for images from different days is not based on an invariant dry edge value as its baseline and it is not convincing to use their respective TVDI values to conclude that the surface from one image is drier than the other. So for this thesis, I mainly addressed three questions: 1) Proposing a more robust surface dryness index for estimating soil moisture; 2) Using this new index to estimate soil moisture to see if there is any trend for soil moisture for a long period of time; 3) Estimate soil moisture and exploring its relationships with land cover and topography.

Therefore, in chapter 2, I addressed my first research question and proposed a more robust surface dryness index, which is based on TVDI, called the Dryness Slope Index (DSI). Then I conducted several experiments to compare the power of TVDI and DSI for estimating surface dryness condition, and proposed an empirical model for estimating soil moisture by using DSI.

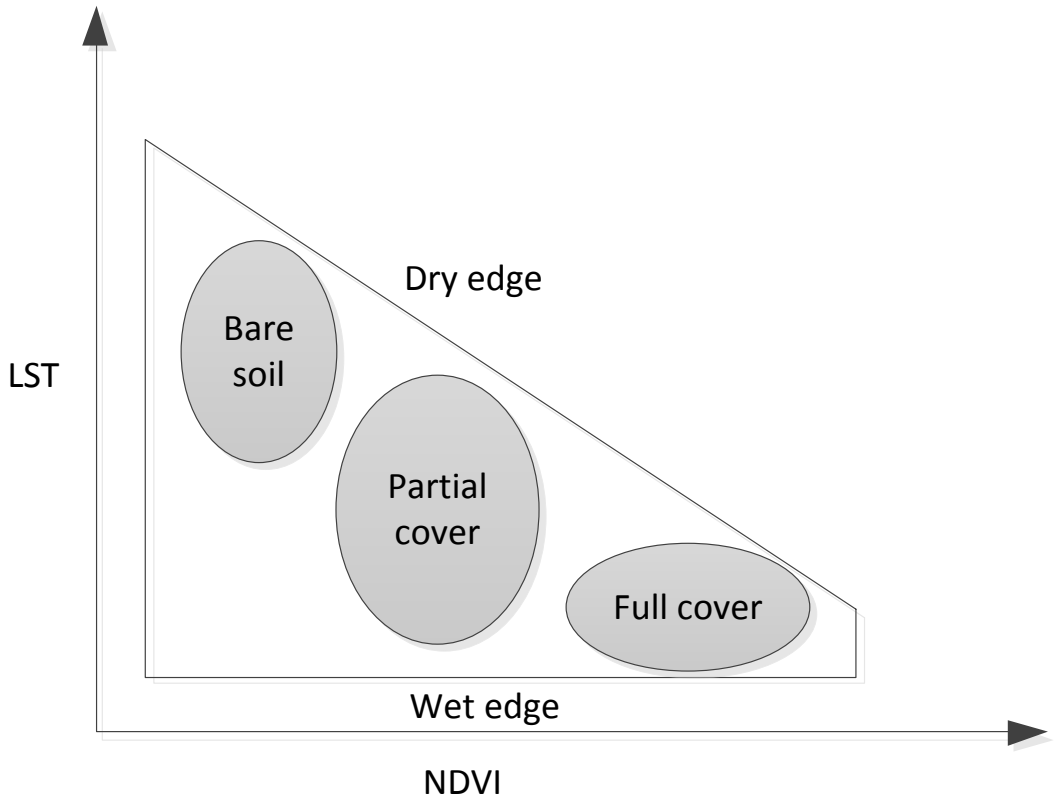

Figure 1.1 LST/NDVI feature space. A scatterplot of remotely sensed surface temperature and a vegetation index often results in a triangular shape, or a trapezoid shape. Bare soil pixels tend to exist in the upper-left corner of the triangle; Full vegetation pixels appear in the bottom-right corner of the triangle; Mixed pixels appear in the center of the feature space.

Soil moisture serves as an essential index for drought prediction and has great implications for agricultural activities and management. Soil moisture dynamics are controlled by many processes including evapotranspiration, infiltration and root water uptake. Changes in land use/cover types are significant anthropogenic factors that influence the spatial distribution of soil moisture, understanding the spatial and temporal relationships between these changes and soil moisture will provide important data that is required to support the efficient use of the available soil moisture and sustainable use of land resource (Wang *et al.*, 2010). Therefore, in chapter 3, I addressed my last two research questions. I analyzed the temporal trend of soil moisture from year 2000 to 2014, and then explored the relationship between soil moisture and several environmental factors, including land cover and topography. In chapter 4, I synthesized the overall findings of this thesis.

References

Ahmad, M. & Bastiaanssen, W.G.M. 2003. Retrieving soil moisture storage in the unsaturated zone using satellite imagery and bi-annual phreatic surface fluctuations. *Irrig. Drain. Syst*., 17:141-161.

Ávila, L.F.; Mello, C.R.; Mello, J.M. & Silva, A.M. 2011. Padrão espaço-temporal da umidade volumétrica do solo em uma bacia hidrográfica com predominância de Latossolos. R. Bras. *Ci. Solo*, 35:1801-1810.

Bezerra, M.V.C.; Silva, B.B.; Bezerra, B.G.; Borges, V.P. & Oliverira, A.S. 2012b. Evapotranspiração e coeficiente de cultura do algodoeiro irrigado a partir de imagens de sensores orbitais. *R. Ci. Agron.*, 43:64-71.

Carlson, Tobyn.; Gillies, Robertr.; Perry, Eileenm. 1994. A method to make use of thermal infrared temperature and NDVI measurements to infer surface soil water content and fractional vegetation cover. *Remote Sensing Reviews* 9(1): 161-173.

Cook, B.I.; Bonan, G.B. & Levis, S. 2006. Soil moisture feedbacks to precipitation in Southern Africa. *J. Climate*, 19:4198-4206.

Hoeben, R., and Troch, P. A. 2000. Assimilation of active microwave observation data for soil moisture profile estimation. *Water Resour. Res*., 36~10, 2805–2819.

Hong Wang, Xiaobing Li, Huiling Long, Xu Xu, Yun Bao. 2010. Monitoring the effects of land use and cover type changes on soil moisture using remote-sensing data: A case study in China's Yongding River basin. *CATENA*. 82(3):135-145.

Kjellström, E.; Barring, L.; Jacob, D.; Jones, R.; Lenderink, G. & Schar, C. 2007. Modelling daily temperature extremes: recent climate and future changes over Europe. *Climatic Change*, 81:249-265.

Kong, X.; Dorling, S. & Smith, R. 2011. Soil moisture modeling and validation at an agricultural site in Norfolk using the Met Office surface exchang scheme (MOSES). *Meteorol. Appl*., 18:18-27.

Lam, **A**.; Karrssenberg, D.; Hurt, B.J.J.M. & Bierkens, M.F.P. 2011. Spatial and temporal connections in groundwater contribuition to evaporation. *Hydrol. Earth Syst. Sci*., 15:2621-2630.

Mattia, F.; Satalino, G.; Pauwels, V.R.N. & Loew, A. 2009. Soil moisture retrieval through a merging of multitemporal L-band SAR data and hydrologic modelling. *Hydrol. Earth Syst. Sci*., 13:343-356.

Oki, T., Nishimura, T., and Dirmeyer, P. 1999. ''Assessment of land surface models by runoff in major river basins of the globe using Total Runoff Integrating Pathways (TRIP).'' *J. Meteorol. Soc. Jpn*., 77, 235–255.

Price, J. C. 1990. Using spatial context in satellite data to infer regional scale evapotranspiration. IEEE *Transactions on Geoscience and Remote Sensing*, 28, 940–948.

Schmugge, **T. J**. 1999. Applications of passive microwave observations of surface soil moisture. *J. Hydrol.*, 212–213, 188–197.

Scott, Christopher A.; Bastiaanssen, Wim G. M.; Ahmad, Mobin-Ud-Din. 2003. Mapping Root Zone Soil Moisture Using Remotely Sensed Optical Imagery. *Journal of Irrigation and Drainage Engineering* 129(4): 326-335.

Seneriviratne, **S.I**.; Luthi, D.; Litschi, M. & Schar, C. 2006. Land-atmosphere coupling and climate change in Europe. *Nature*, 443:205-209.

Ulaby, F. T., and Elachi, C., eds. 1990. Radar polarimetry for geoscience applications, Artech House, London.

Verhoest, N. E. C., Troch, P. A., Paniconi, C., and de Troch, F. P. 1998. Mapping basin scale variable source areas from multitemporal remotely sensed observations of soil moisture behavior. *Water Resour. Res*., 34~12, 3235–3244.

Vischel, T.; Pegram, G.G.S.; Sincair, S.; Waner, W. & Bartsch, A. 2008. Comparison of soil moisture fields estimated by catchment modeling and remote sensing: A case study in South Africa. *Hydrol. Earth Syst. Sci.*, 12:751-767.

Vivoni, E.R.; Entekhabi, D.; Bras, R.L. & Ivanov, V.Y. 2007. Controls on runoff genration and scale-dependence in a distributed hydrologic model. *Hydrol. Earth Syst. Sci*. 11:1683-1701.

Walker, J. P., and Houser, P. 2001. A methodology for initializing soil moisture in a global climate model: Assimilation of near-surface soil moisture observations. *J. Geophys. Res*., 106, 11761–11774.

Chapter 2 - The Dryness Slope Index (DSI) – A Modified Form of the Temperature Vegetation Dryness Index (TVDI) for Estimating Soil Moisture

Abstract

Soil moisture is an important biophysical property of soil, which controls energy exchange, evapotranspiration, vegetation coverage at the surface. Various methods have been proposed to estimate soil water content based on field investigations, active/passive microwave remote sensing and optical/thermal remote sensing among which the "triangle" method and the notion of TVDI have been frequently used to retrieve soil moisture. In this study the assumptions of the "triangle" method were examined by using the Surface Energy Balance System model (SEBS). A form of modified form of TVDI, the Dryness Slope Index (DSI), is proposed and evaluated. TVDI and DSI have been calculated for different images, and the spatial pattern and temporal evolution of TVDI and DSI has been explored and compared with the meteorological data. The results showed that TVDI and DSI do a good prediction in the spatial distribution of soil moisture, where vegetated areas showed more soil water content and less vegetated areas showed less soil moisture. However, TVDI presented a poor match with the meteorological data after rainy days, which showed higher TVDI values than drier days, on the other hand DSI showed more reasonable match with the meteorological data. The Willmott index of agreement was then used to verify if there was a uniform relationship between DSI and evaporative fraction (EF) on different images, and results showed that a statistically significantly uniform relationship was found between DSI and evaporative fraction among different images, meaning that DSI is less susceptible to sudden rainfall and is a more robust surface dryness index. In the end, an empirical model for estimating soil moisture was proposed by using DSI.

Key words: the "triangle" method, TVDI, the dry edge and wet edge, slope of soil moisture isolines, the dryness slope index, evaporative fraction

Introduction

Soil moisture is an important factor that controls energy exchange between the land and the atmosphere, and is also an important indicator for drought and agricultural management. The spatial and temporal distribution of soil moisture strongly influences the surface heat balance, evapotranspiration, and soil temperature. Acquisition of data on land surface energy exchanges is an important part of monitoring changes in regional resources and environments. Since soil moisture plays such a significant role in these exchanges, large-scale monitoring of soil water levels can play a vital role in agricultural research and environmental evaluations. Retrieval of soil moisture values at regional or global scales is therefore an important tool in studies of land surface processes (Moran *et al*., 1994).

Water content in soil and vegetation can be estimated using three methods: (1) field measurements; (2) meteorological data; and (3) remote sensing. Although field measurements can provide the most accurate information on soil and vegetation water content, they are expensive and time consuming especially for mountainous or remote areas. What's more, the spatial distribution of soil moisture based on interpolation of the point-based data has limited frequency and spatial coverage of field investigations. There are several climatic and hydrological drought indices (point-based) which are based on meteorological data. However, point-based data are often poorly distributed and are insufficient and not available for timely water stress/drought detection.

Technological advances in satellite remote sensing offer an alternative to studying soil moisture and enabled us to monitor it at higher temporal and spatial resolutions at lower cost and time. Since the 1970s a number of remote sensing methods have been developed to investigate soil moisture by using different regions of electromagnetic spectrum including the microwave, thermal, and the optical (Carlson *et al*., 1995a; Gillies and Carlson, 1995b). Comprehensive reviews on the applications of remotely sensed methodologies for the estimation of surface water content including the principles, advantages and constraints can be found in the study of Verstraeten *et al*. (2008).

The main disadvantage of current methods to estimate soil moisture from passive microwave techniques is its coarse spatial resolution (around 40 km) making it difficult to study finer scale variations in an appropriate manner (Merlin *et al*., 2010). Therefore, there are demands for the development of approaches to downscaling soil moisture data from low spatial resolution

microwave sensors. Optical/thermal remote sensing data provide finer spatial and temporal resolution information that can be used to improve passive microwave estimations on soil moisture. Efforts are being made to downscale passive microwave soil moisture estimations using optical/thermal infrared data (Chauhan *et al*., 2003) but downscaling methodologies still need to be improved. Even though airborne passive radiometers are able to provide soil water information at higher spatial resolution, frequent flights are infeasible and often unaffordable. There are several active microwave sensors in the form of radars aboard on the RadarSat, EnviSat, the European remote sensing (ERS) satellite, Japan Earth resources (JERS) satellite, which provide observations at 20 ~ 30 meter spatial resolution. The Soil Moisture Active Passive (SMAP) was launched 31 January 2015 by NASA. It can provide measurements of the land surface soil moisture and freeze-thaw state with near-global revisit coverage in 2 ~ 3 days. It carries a radiometer that records microwave emissions from the top 5 cm in the soil with a spatial resolution of about 40 km, and radar will provide backscatter measurements at 1 km resolution. However, the ERS, JERS, and the radar of SMAP are no longer operational. What is more, active microwave sensors have limited ability to penetrate the vegetation layer and the backscatter coefficient is significantly affected by surface roughness (Ulaby and Elachi 1990; Verhoest *et al*. 1998; Hoeben and Troch 2000).

Optical/thermal remote sensing provides an alternative approach to remote sensing soil moisture, with the potential for relatively high spatial/temporal resolution and availability compared to microwave remote sensing data. In the visible and near-infrared wavelengths, the radiation and reflection characteristics of the surface largely depend on the spectral response of vegetation and soil for a natural surface. The soil moisture status influences chlorophyll content in the leaves and in turn changes the spectral response of vegetation. Similarly, soil water content also affects the spectral response of soil as it is known that soil reflectance decreases with increasing soil water content. In the thermal infrared wavelengths, land objects vary in terms of temperature and emissivity, which is largely controlled by their thermal inertia. Soil moisture can therefore influence the temperature of vegetation and surface soil. Water content changes in chlorophyll because of the change of soil moisture can be detected in terms of variations of vegetation indices such as NDVI. However, NDVI is a rather conservative indicator of water stress as vegetation remains green after initial water stress. However, the surface temperature can rise rapidly with water content decreasing. Therefore, land surface temperature and vegetation indices in combination can provide more comprehensive information on water content at the surface, and

number of surface dryness indices have been developed based on visible and thermal band of remotely sensed data. Zhan *et al*., (2007) proposed the model of soil moisture monitoring by remote sensing (SMMRS) based on the near-infrared versus red spectral reflectance feature space from which evaporative fraction is derived, and SMMRS is calculated by subtracting evaporative fraction from 1 which represents the soil moisture of completely wet soil. Wang *et al*., (2007) proposed the Normalized Multi-Band Drought Index (NMDI) by using the apparent reflectance observed from MODIS at 860 nm, 1640 nm and 2130 nm owing to the fact that channels centered at 1640 nm and 2130 nm can reflect strong differences between two water absorption bands in response to soil and leaf water content, giving this combination potential to estimate water content for both soil and vegetation. Wang *et al*., (2010) estimated soil moisture by utilizing the vegetation dryness index (TVDI) and an empirical linear model which describe the relationship between in situ soil moisture observations and TVDI values.

In the 1990s, a new approach, for mapping both land surface moisture and surface turbulent energy fluxes gained popularity (Price, 1990, Carlson *et al*., 1994). This method, referred to here as the triangle method, allows the pixel distribution from the image to fix the boundary conditions for the model, thereby largely bypassing the need for ancillary atmospheric and surface data. There have been many proposed surface dryness indices based on the triangle method and TVDI. Rahimzadeh *et al*., (2011) modified TVDI by incorporating the Digital Elevation Model (DEM) and air temperature. Gao *et al*., (2010) explored the possibility of combination TVDI with various vegetation indices and evaluated their performance in estimating soil moisture. However, few studies have been done to examine the theoretical basis of the "triangle" method. Therefore, in this paper I aimed to test the assumptions of the "triangle" method using a Surface Energy Balance System model (SEBS, Su 2001), then proposed a modified form of TVDI, the Dryness Slope Index (DSI) based on the examination of its theoretical basis.

Background and Objectives

The triangle method is based on an interpretation of the pixel distribution in the LST/NDVI feature space. LST is affected by many factors such as surface thermal properties, net radiation, evapotranspiration, and vegetation coverage, hence there is no direct relationship between LST and soil water content. However, soil moisture is an important factor controlling vegetation canopy temperature and under certain vegetation coverage soil moisture can indirectly affect canopy temperature. The LST/NDVI feature space (shown in Figure 2.1) is used to illustrate the relationship among LST, soil moisture and vegetation coverage. A scatterplot of remotely sensed surface temperature and a vegetation index often results in a triangular shape (Price, 1990; Carlson *et al*., 1994), or a trapezoid shape (Moran, Clarke, Inoue, *et al*., 1994) if a full range of fractional vegetation cover and soil moisture contents is present in the data. Previous studies (Prihodko and Goward 1997; Moran *et al*. 1994; Carlson *et al.* 1995; Gillies *et al*. 1997; Sandholt *et al.* 2002) have shown that the triangular feature space consists of a family of soil moisture isolines, which are also TVDI isolines, representing different degrees of aridity, and isolines closer to the upper boundary of the feature space represent pixels with low soil moisture. The horizontal line at the low limit in the LST/NDVI feature space is called the wet edge (unlimited water availability) while the sloping line is called the dry edge (maximum evapotranspiration and limited water access). There are three assumptions behind the triangle method and the use of TVDI, which are 1) The feature space of land surface temperature (LST) and NDVI results in a triangular shape given a large number of pixels reflecting a full range of soil surface wetness and vegetation coverage. The boundaries of the triangle reflect real physical limits: day bare soil, full vegetated surface, wet bare soil, and driest condition in the frame; 2) The LST/NDVI feature space consists of many soil moisture isolines which are also TVDI isolines; 3) The upper boundary of the triangle represents the driest condition in the frame, and the lower limit reflects soil with unlimited water availability (at field capacity or above). A dryness index is proposed from the LST/NDVI feature space to describe the relationship among the three and it is calculated as the ratio of A to B for point C in the feature space:

$$TVDI = \frac{T_c - T_{min}}{T_{max} - T_{min}} = \frac{A}{B} \qquad (1)$$

where T_c represents the land surface temperature of a pixel; T_{min} is the temperature at the wet edge; T_{max} represents the temperature at the dry edge under the same NDVI and is calculated as $T_{max} = a + b * NDVI$, where a and b are the coefficients of the regression equation for the dry edge. According to the definition of TVDI, values at dry edge would be 1 and at the wet edge, 0. Larger TVDI values thus indicate drier soil.

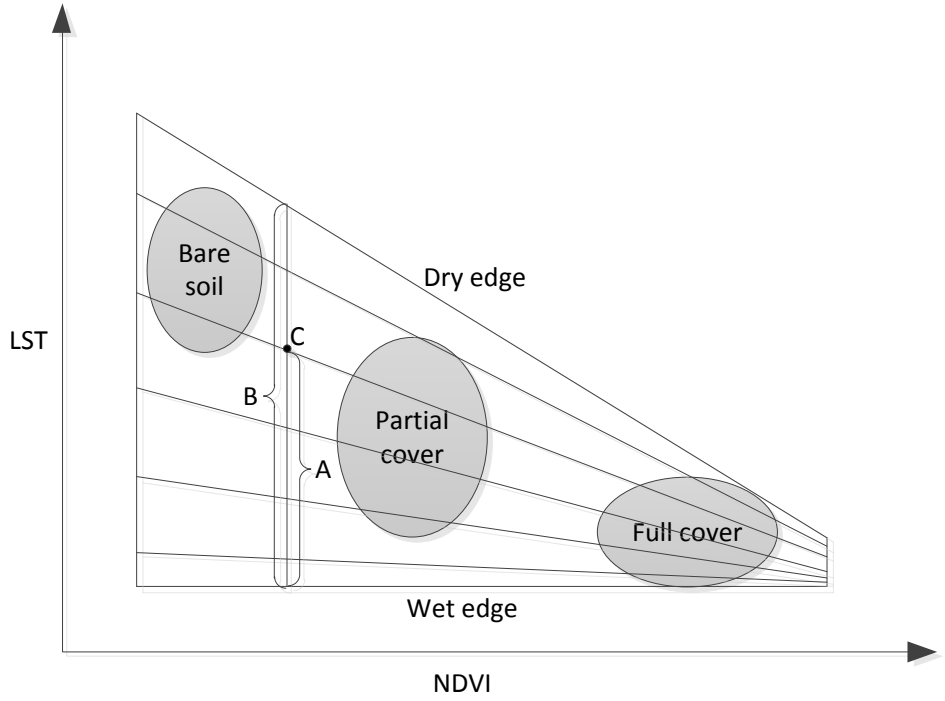

Figure 2.1 LST/NDVI feature space. Bare soil pixels tend to exist in the upper-left corner of the triangle; Full vegetation pixels appear in the bottom-right corner of the triangle; Mixed pixels appear in the center of the feature space. For pixel C, its TVDI value calculates as the ratio between A (the distance from its LST value to the wet edge) and B (the distance between the maximum LST under the same NDVI to the wet edge). The slanting lines within the LST/NDVI feature space are TVDI isolines.

Even though the triangle method and TVDI have been widely used to estimate surface dryness condition, few studies have been carried out to the theoretical basis of the triangle method, and the use of TVDI without extra attention may lead to incorrect conclusions especially when comparing the dryness condition of several different dates by comparing their perspective TVDI values. To illustrate, consider the following situation: (a) represents the LST/NDVI feature space of dry day and (b) imitates the feature space of a day after receiving rainfall (See Figure 2.2). Because of the rainfall the temperature difference between the maximum and minimum LST in (b) is likely to be smaller than that of the feature space in (a). Assuming the two dates are close so that there is little difference in terms of their NDVI range, then the size of feature space of (a) is bigger than that of (b). As a result, for pixels having similar NDVI values, it is likely that the ratio between bc and ac is larger than the ratio between BC and AC, indicting TVDI values for a wetter surface are larger than that of a drier surface.

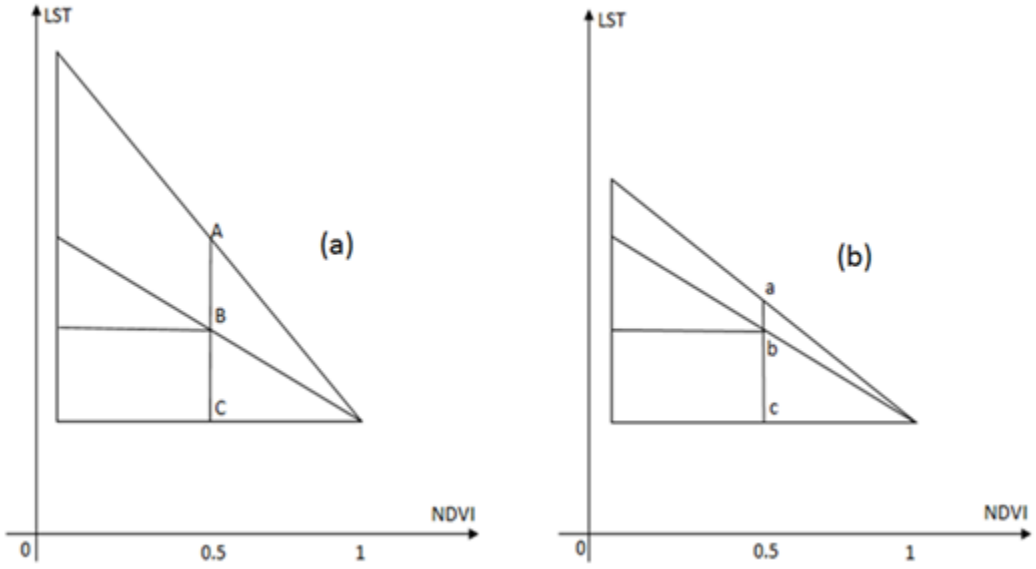

Figure 2.2 Example LST/NDVI feature space of a dry surface and a wet surface. (a) imitates the feature space of a dry day, where the LST/NDVI feature space is larger than the feature space of the day after receiving rainfall, such as (b). For pixels that have similar NDVI values, it is likely that the ratio between bc and ac is larger than the ratio between BC and AC owing to the fact the feature space of (b) is smaller than that of (a), indicting TVDI values for a wetter day will be greater than that of a drier day.

This inconsistency is caused by how TVDI is defined. Recall that TVDI is based on the position of the dry edge and that of the wet edge. The former, represents the driest condition in the frame, does not necessarily means that soil moisture is zero and is likely to vary for images from different days, whereas the latter has a fairly stable physical meaning which is at field capacity or above. So, the calculation of TVDI for images from different days is not based on an invariant dry edge value as its baseline and it is not convincing to use their respective TVDI values to conclude that the surface from one image is drier than the other.

From the above analysis, we can see that it is of significance to examine the theoretical basis of the triangle method on which TVDI is based before it can be applied. To achieve this goal, I first used the SEBS model to study the LST/NDVI feature space and their relationship. Then in order to avoid the problem of TVDI from different days having different basis, I proposed a modified surface dryness index, called the Dryness Slope Index (DSI), based on TVDI. In order to compare the power of TVDI and DSI for estimating surface dryness condition, I conducted several experiments at the Konza Prairie Bilogical Station (KPBS) using Landsat5 TM images and meteorological data from the KPBS. To be specific, I compared the spatial and temporal pattern of soil moisture using TVDI and DSI, and I then used Willmott's d index of agreement (Willmott *et al. 1980*) to test if DSI can be applied to estimate soil moisture across different images. In the end, I formulated an empirical model for estimating soil moisture using DSI.

Study area and data

The study area (See Figure 2.3) is mainly located at the Konza Prairie Biological Station (KPBS). KPBS is a 73 km^2study area is located in south of Manhattan, Kansas. It is a member of the National Science Foundation's Long Term Ecological Research (LTER) network, and thus maintains an extensive archive of ecological and climatological data supporting this research. The site includes both native prairie and some agricultural land. The main land cover is grassland, forest, cultivated crops, barren land and open water. Except for agricultural lands whose land cover type varies throughout a year, other land cover types remain relatively stable. Around 76% of annual rainfall (835mm) occurs during the growing season, and it is highly variable from year to year. The main soil types in the study area are silt loam and silty clay loam.

Landsat5 TM images are used for its relatively high spatial and temporal resolution. To be specific, fourteen Landsat5 TM images from May to the early October for 2007 and 2008 were selected for this analysis, using two criteria: 1) The vegetation has turned green from May and remained to be so till October; 2) they have the longest cloud-free images series. Images acquired are listed below (See Table 2.1).

Table 2.1 Dates of Landsat5 TM images

2007		**2008**	
May 18, 2007	LT50280332007138PAC01	May 4, 2008	LT50280332008125PAC01
May 25, 2007	LT50280332007154PAC01	May 20, 2008	LT50280332008141PAC02
July 21, 2007	LT50280332007202PAC01	June 21, 2008	LT50280332008173PAC01
August 6, 2007	LT50280332007218PAC01	July 23, 2008	LT50280332008205PAC01
August 22, 2007	LT50280332007234PAC01	August 8, 2008	LT50280332008221PAC01
Sep 7, 2007	LT50280332007250PAC01	Sep 9, 2008	LT50280332008253PAC01
Sep 23, 2007	LT50280332007266PAC02	Sep 25, 2008	LT50280332008269PAC01

The required input data for running the SEBS model come from two sources: Landsat5 images (to estimate LST, NDVI, emissivity, albedo) and meteorological data from KPBS (wind speed, air temperature and pressure, and relative humidity *etc*). Additional ancillary data for validation purposes includes precipitation data, daily evapotranspiration data and so on.

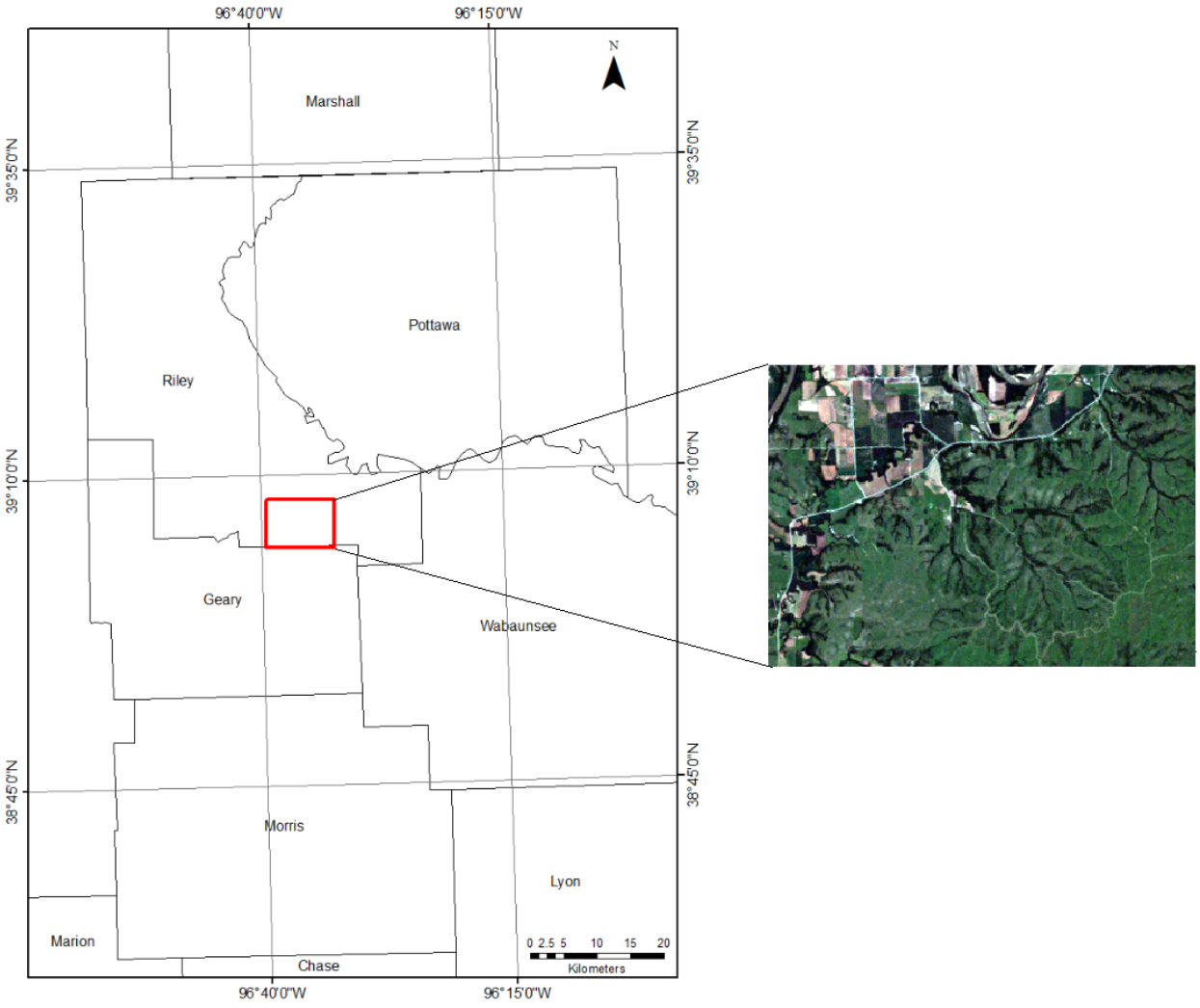

Figure 2.3 Study area (marked by the red rectangle)

Methods

Surface energy balance system model (SEBS)

The SEBS model (Su 2001) is a physically based energy balance model which consists of three main parts: 1) methods for the determination of the physical and biological parameters of the surface, such as albedo, emissivity, temperature, and vegetation coverage, 2) a model for the determination of the roughness length for heat transfer, and 3) a formulation for the determination of the evaporative fraction on the basis of energy balance at limiting meteorological conditions. At dry limiting condition the latent heat becomes zero due to the limitation of soil moisture, while the sensible heat flux is at its maximum value. Estimation of evaporative fraction requires both dry and wet limiting conditions. Under the wet limiting condition, the evaporation takes place at its maximum rate. The model calculates instantaneous relative evaporation as:

$$\Lambda_r = 1 - \frac{H - H_{wet}}{H_{dry} - H_{wet}} \qquad (2)$$

where H_{wet} is sensible heat flux (W/m^2) under the wet limiting condition where ET takes place at maximum rate. H_{dry} is the sensible heat flux at the dry limiting condition where ET is zero due to limited soil moisture. The evaporative fraction is calculated as:

$$\Lambda = \Lambda_r * (1 - \frac{H_{wet}}{H_{dry}}) \qquad (3)$$

Where Λ is the evaporative fraction. The data needed for running SEBS model and their source is listed in below (See Table 2.2).

Table 2.2 Main variables for running the SEBS model

Variable Name	Data Source
land surface temperature, land surface albedo, emissivity, NDVI	estimate from Landsat TM 5
vegetation fraction, leaf area index	calculated in SEBS
Digital Elevation Model (DEM)	SRTM DEM data
sun zenith angle, reference height	KPBS
wind speed, air temperature, mean daily air temperature,	KPBS
pressure at reference height, pressure at surface map, sunshine hours	KPBS
horizontal visibility, planetary boundary layer height	empirical data

The Integrated Land and Water Information System (ILWIS, version 3.8, Allard *et al*, 1988) was used to run the SEBS model. According to Scott *et al*. (2003) who proposed a way to estimate soil moisture:

$$\theta = \theta_{sat} * e^{(\Lambda - 1)/0.42} \qquad (4)$$

where θ_{sat} is the saturated soil moisture. According to equation 4 that, we can see that pixels with same evaporative fraction (EF) values, which can be calculated from SEBS model, with similar soil composition would have similar soil water content. Since NDVI and LST are two inputs of the SEBS model, we are then able to explore the relationship between the two under different evaporative faction values, which can be estimated from the SEBS model.

TVDI for estimating surface dryness condition

According to equation 1 that TVDI is defined as:

$$TVDI = \frac{T_c - T_{min}}{T_{max} - T_{min}} \quad (5)$$

where T_c represents the land surface temperature of a pixel; T_{min} is the temperature at the wet edge; T_{max} represents the temperature at the dry edge under the same NDVI and is calculated as $T_{max} = a + b * NDVI$, where a and b are the coefficients of the regression equation for the dry edge. According to the definition of TVDI, the TVDI value at dry edge would be 1 and that at the wet edge is 0.

A modified form of TVDI ---- the Dryness Slope Index (DSI)

From the previous analysis, we can see that TVDI is based on the dry edge as well as the wet edge. The former, represents the driest condition in the frame, varies for different images, whereas the latter has a fairly stable physical meaning which is at field capacity or above. As we recall, the LST/NDVI feature space consists of a family of soil moisture isolines which are also TVDI isolines, and drier pixels correspond to steeper soil moisture isolines, whereas the wetter pixels have less steep isolines. Since the slope of the soil moisture isolines is confined in the specific feature space and its maximum value is not larger than the slope of the dry edge, we can then use the slope of soil moisture isolines as a measurement to show how far each soil moisture isoline is deviated from the wet edge, thus we have the same basis for measuring soil moisture when across different images. From the above analysis, DSI is defined as the absolute value of the slope of each soil moisture isoline, and the formulation of this index is calculated as:

$$DSI = |a * TVDI| \quad (6)$$

where a is the slope of the dry edge for a specific frame; TVDI is the TVDI value for each pixel within the same frame. Since the slope of the dry edge is negative, we take the absolute value to show how far a soil moisture isoline is deviated from the wet edge. As a result, drier pixels would be further from the wet edge and thus have larger DSI values.

Results

SEBS output and the relationship between NDVI and LST

The SEBS model was used to calculate evaporative fraction for several images (taking image 2008221 as an example), and the results are summarized as below (See Figure 2.4). We can see that points, which have similar evaporative fraction (EF) value, correspond to a family of NDVI and LST points that are highly correlated, which means that soil moisture isolines are linear in the LST/NDVI feature space. The results also show that the pixels corresponding to steeper isolines have less water content as they show low evaporative fraction values. The pixel set with EF value around 0.04 almost represents the driest condition in the frame, and it has the steepest slope. The soil becomes wetter as the EF increases and the slope of the isolines become less steep. Each point set covers a fairly large range of NDVI and LST, meaning different NDVI and LST combinations can represent soil with similar water content. The above results show that the assumptions of the triangle method are verified to be valid by exploring the relationship between LST and NDVI under different soil moisture conditions with the help of the SEBS model.

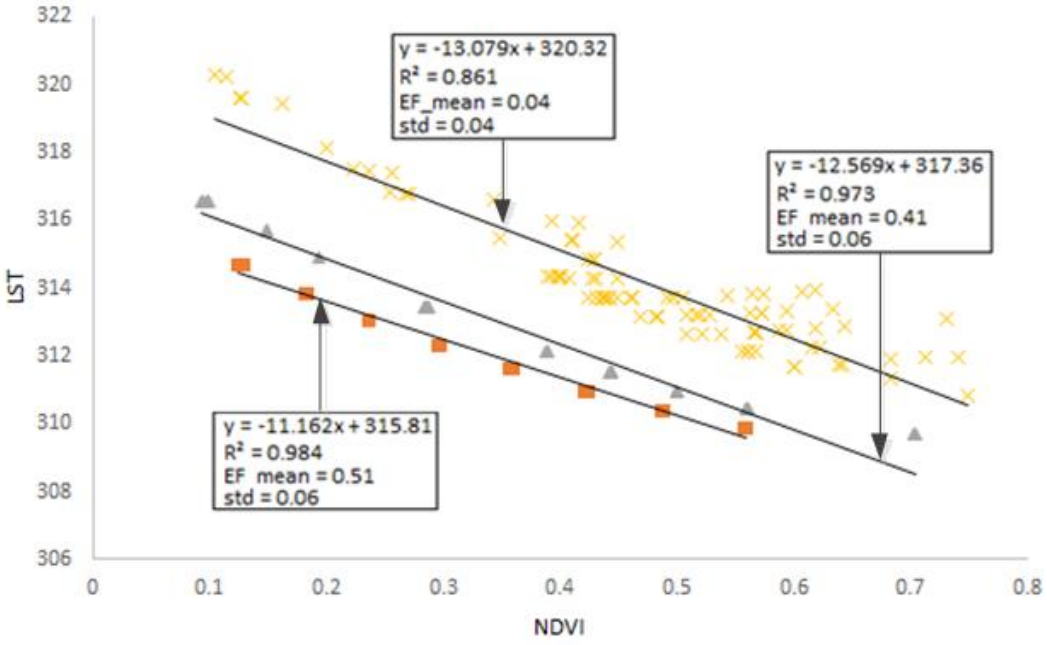

Figure 2.4 LST/NDVI feature space under different EF conditions

Plots of LST/NDVI feature spaces

In order to determine the parameters for the dry edge, the maximum temperature observed for small intervals of NDVI is extracted in the feature space, and then least square regression is used to estimate the slope and intercept of the dry edge (Figure 2.5, also see Appendix[1]). The lowest temperature in the feature space was regarded as the wet edge. TVDI variables, including dry edge slope, intercept and wet edge, for the 14 images from 2007 and 2008 are shown below (Figure 2.6). By comparing with the precipitation data through May to October, we can see that the variables are closely associated with the amount of rainfall being received. Days after rainfall often coincide with lower wet edge position, and less steep dry edge. For example, the day 2007154 and 2008253 have the least steep dry edge because rainfall happened shortly before these days. Steep dry edge slope and high wet edge position often correspond to dry days, such as the day 2007202 and the day 2008125, 2008141. Generally speaking, the relationship between the TVDI parameters and rainfall is that drier weather conditions often mean a steeper dry edge and higher wet edge position, and days after receiving rainfall show the opposite. Thus, it is reasonable to use the triangle parameters as an indicator of soil wetness condition. The LST/NDVI feature space is poorer-defined during rainy days, such as the day 2008253 since the day before, which is 2008252, 42.3mm rainfall was recorded. This is probably because there are few dry soil pixels in the frame because of the rainfall.

[1] The Python codes for calculating TVDI and DSI is attached in Appendix

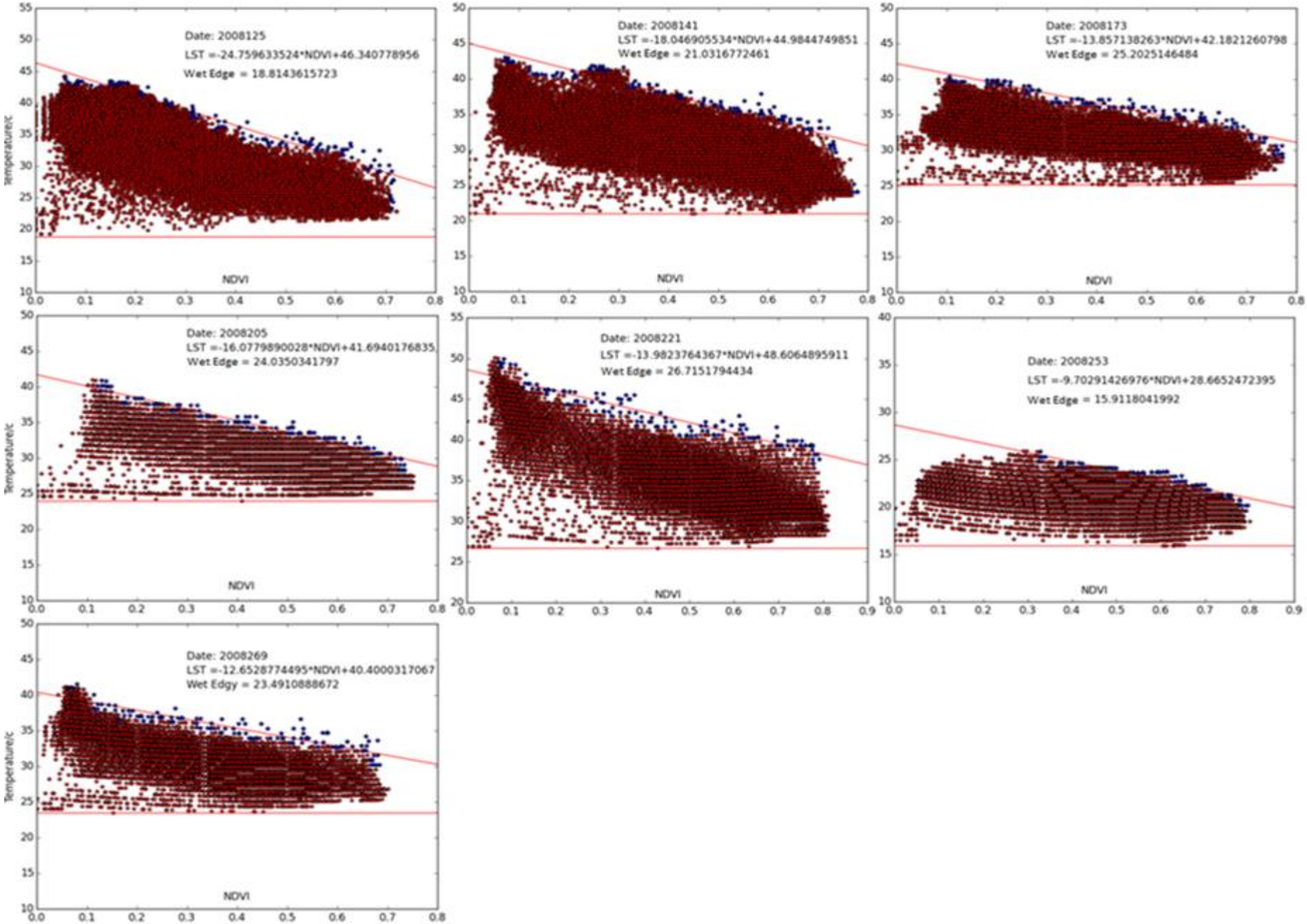

Figure 2.5 LST/NDVI feature space of selected images in 2008

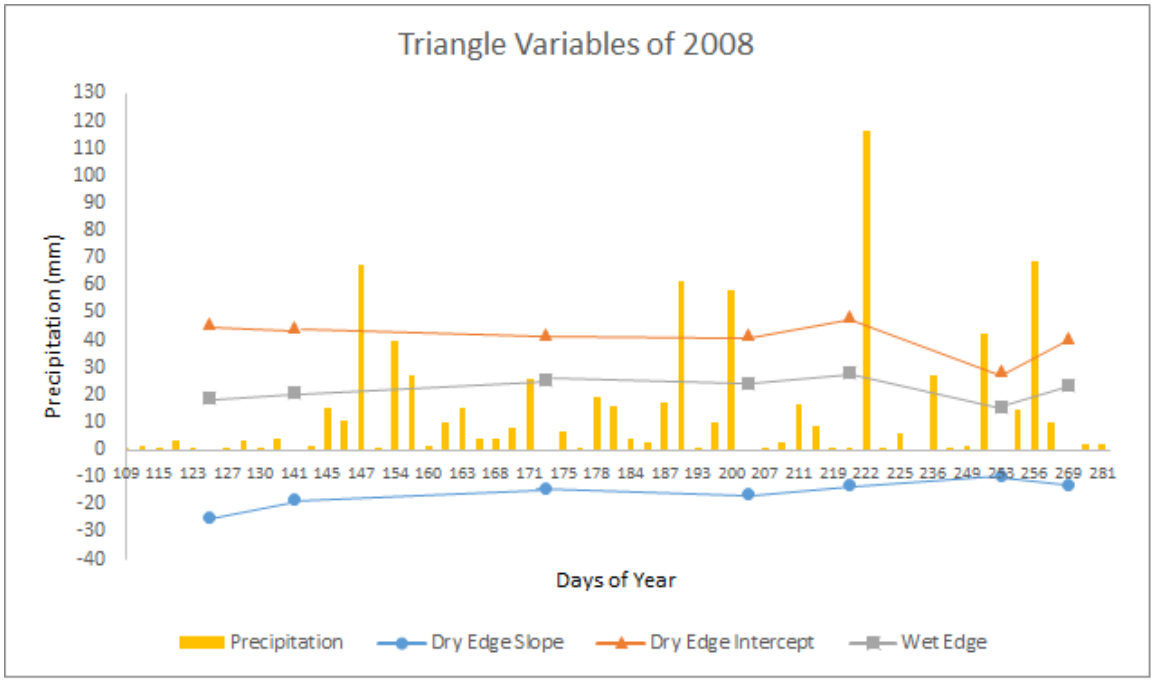

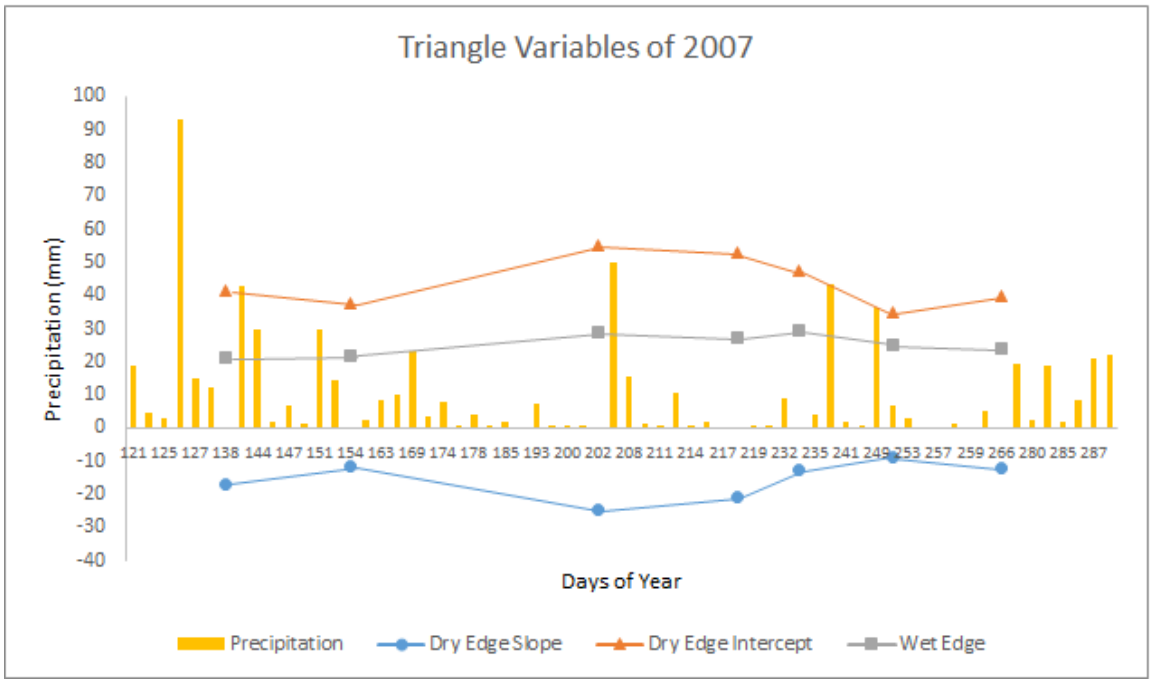

Figure 2.6 Triangle variables temporal evolution in 2007 and 2008

Spatial distribution of TVDI and DSI

From the theoretical discussion about the LST/NDVI feature space, it is apparent that vegetated areas tend to have lower TVDI and DSI values indicating high soil water content, while less vegetated areas are more likely to be drier and have higher TVDI and DSI values. Taking the image 2008221 as an example (See Figure 2.7), the drainage systems (illustrated as A) at Konza tend to have low TVDI and DSI value because it is densely covered by vegetation. Places around the drainage in Konza are covered by grass, and they have higher TVDI and DSI value. Agricultural lands (B) in the north of Konza have high TVDI and DSI values because it is bare soil and not covered by crops. The west of Konza (shown as C) has higher TVDI and DSI values than the east as it is less vegetated.

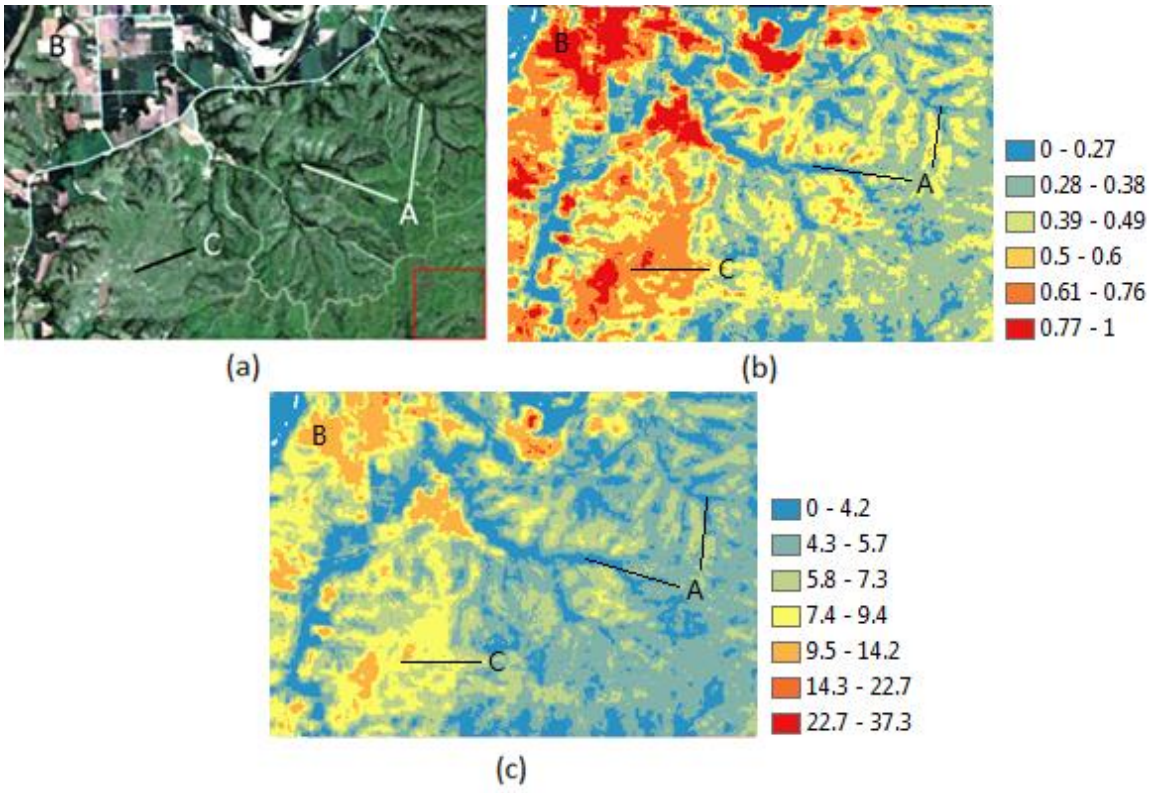

Figure 2.7 Spatial distribution of TVDI of 2008221 (August 8, 2008). (a) is a true-color image from the study area; (b) and (c) are the TVDI image and DSI image, respectively, for the same area.

Temporal evolution of TVDI and DSI

A comparison of TVDI and average precipitation at 9 sites at KPBS (see Figure 2.8), suggests that TVDI is, in general, sensitive to rainfall, and the index drops after rainfall. For example, in 2008 from the period of day 109 to 145, which received little rainfall, and as a result day 125 and day 141 show the high TVDI values. Day 173 has lower TVDI value than the previous two after receiving rainfall. However, there is one abnormality to be noted. The day 2007249 received 36.2 mm rainfall, and the soil would be wet and the day after that (2007250) should have lower TVDI values than day 2007218 which is in the middle of dry period. Similarly, the day 2008252 received 42.3 mm rainfall; however, the TVDI value of the day 2008253 is almost the highest for the year even compared to the driest period, which is from the day 2008109 to 2008145. However, the temporal evolution of DSI present a more reasonable match with the rainfall data. We can see that the day 2007205 and the day 2008253, which received significant rainfall the day before and have shown high TVDI values, show lower DSI values, indicating that DSI has a better explanatory power in the temporal change of soil wetness condition.

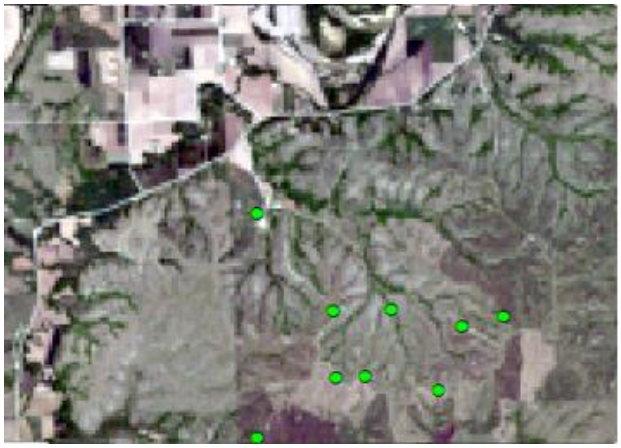

Figure 2.8 Location of comparison sites for precipitation and TVDI at KPBS. The indicated sites are locations of rain gauges from the Konza USGS weather and stream gauging station.

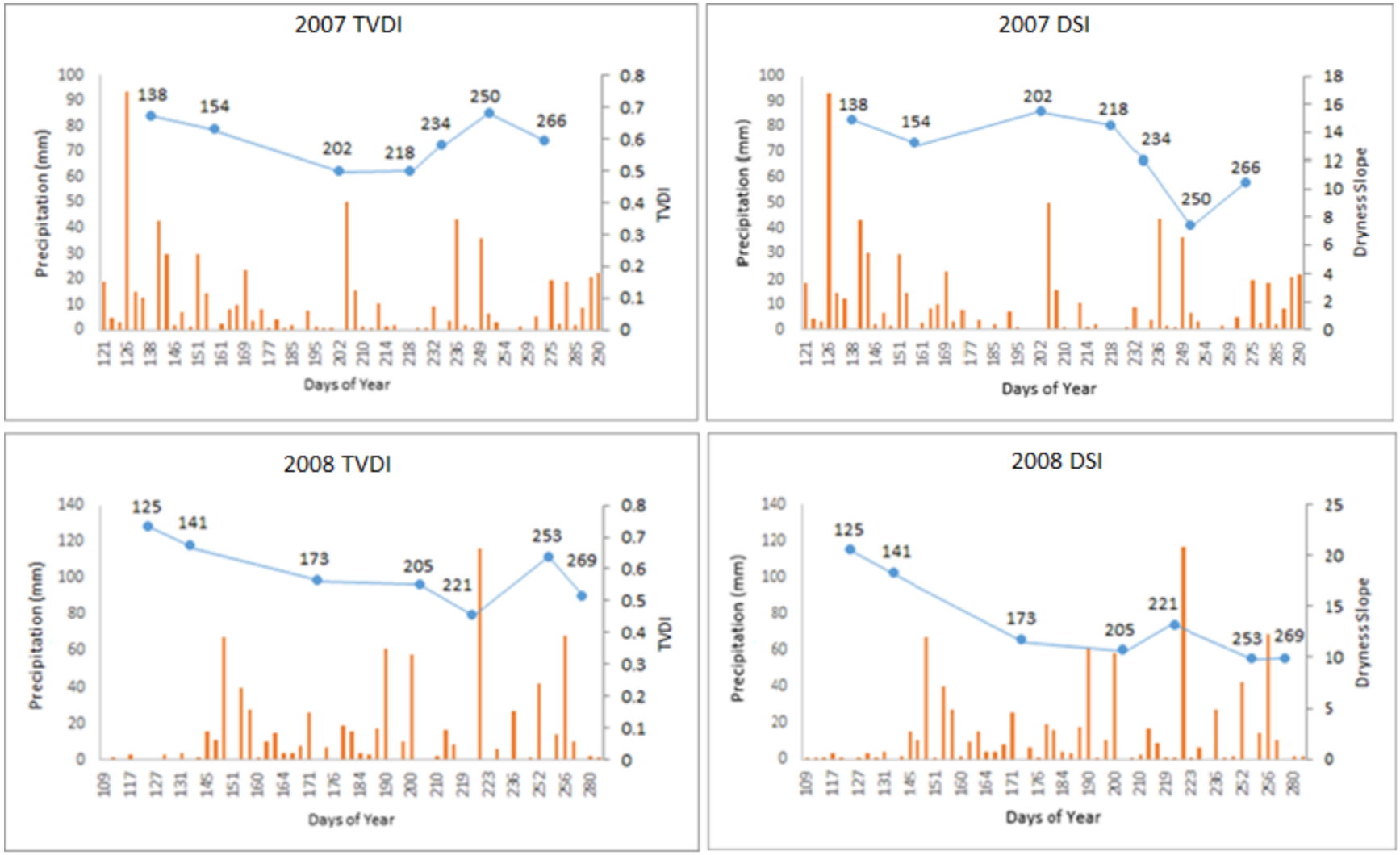

Figure 2.9 Temporal evolution of DSI and TVDI

Validation of DSI across dates

Having concluded that DSI is less sensitive than sudden rainfall than TVDI, I am going to use DSI as an index of surface dryness index. In order to test if there is a uniform relationship between DSI and evaporative fraction, four different images were chosen to validate DSI, including two dates (2007250, 2008205) whose NDVI/LST feature space are well-defined and two other dates (2008221, 2008253) whose NDVI/LST feature space are more poorly defined. The LST/NDVI feature spaces of these four dates are shown below (See Figure 2.10).

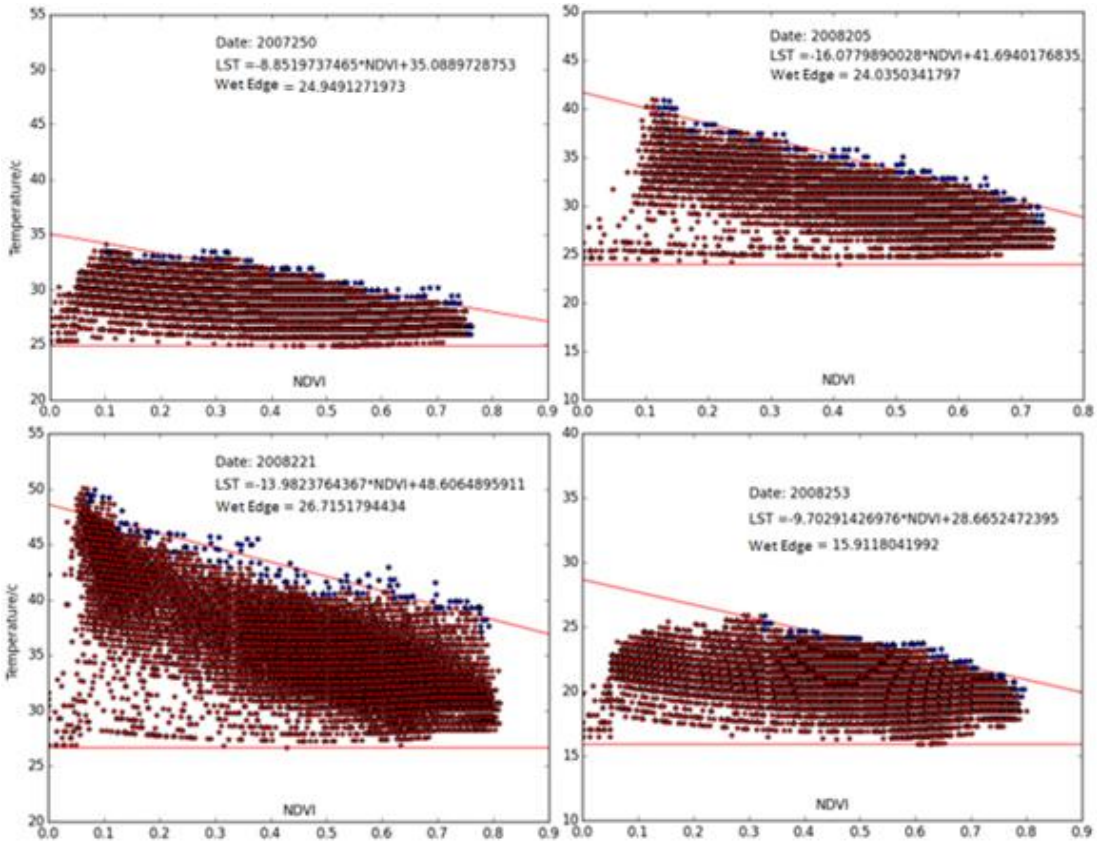

Figure 2.10 LST/NDVI feature space of the selected dates

The SEBS model is used to estimate evaporative fraction for these four dates and they are plotted against DSI and a line is fitted to each plot (shown in Figure 2.11, regression equation, R square and p value are also given). To assess the agreement among four regression lines the Willmott index of agreement is used. Willmott *et al.* (1980) developed the index of agreement (d), which was used to validate the developed forecasting models. The index of agreement (d) is expressed by the following equation:

$$d = 1 - \frac{\sum(P_i - O_i)^2}{\sum(|P_i - \overline{O}| + |O_i - \overline{O}|)^2} \qquad (7)$$

where P_i is the prediction value, O_i is the observed value and $\overline{O}$ is the mean of the observed value. The optimum value of d is 1 meaning that all the modeled values fit the observations.

DSI values ranging from 0 to 20 with an interval of 0.1 (201 points for each set) are chosen to produce the corresponding EF values for each regression equation. Four sets of EF values are compared with one another using the Willmott index of agreement, and the results are shown below (See Table 2.3).

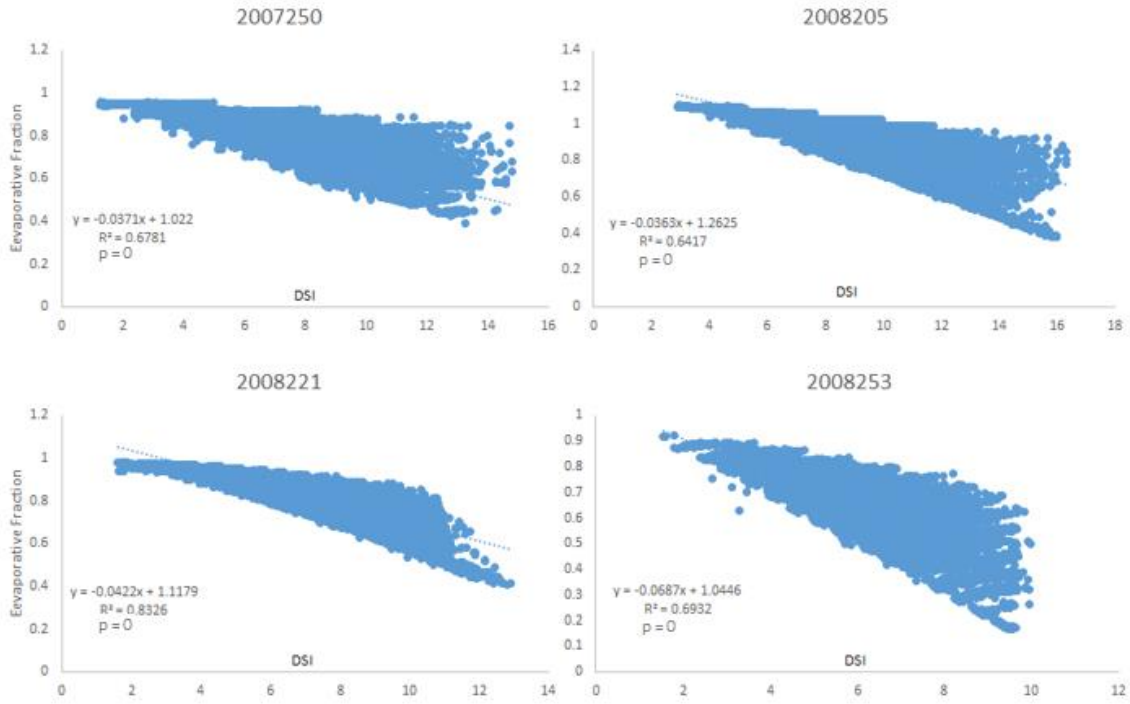

Figure 2.11 EF/DSI plot for the selected dates

Table 2.3 Willmott index of agreement for each EF pair

	2007250	2008205	2008221	2008253
2007250	1	0.7592	0.9865	0.7628
2008205		1	0.9357	0.6223
2008221			1	0.7611
2008253				1

From the d values above it is apparent that the regression equations from the day 2007250 and 2008221 as well as 2008205 and 2008221 produce a good fit (with d value greater than 0.9) between each other. Regression equations for the day 2007250 and 2008205, 2007250 and 2008253, 2008221 and 2008253 produce a fairly good agreement (with d value greater than 0.75) between each other. The worst agreement is seen between 2008205 and 2008221 whose d value is slightly larger than 0.60. The good agreement indicates that there is a uniform regression equation, which can be used to estimate evaporative fraction based on DSI values, and according to equation 4 that soil moisture can be expressed as (taking the regression equation from the day 2008221):

$$\theta = \theta_{sat} * e^{(-0.442*\mathrm{DSI}+0.1179)/0.42} \quad (8)$$

where θ_{sat} is the saturated soil moisture.

Discussion and Summary

Soil moisture is an important index about energy exchange between the land and the atmosphere and it is related to evapotranspiration, vegetation, soil heat balance and so on. Great efforts have been made to estimate soil water content using various ways. Soil moisture probes can provide the most accurate information about soil water content but it is limited by high costs, labor and the inability of investigating large and remote areas. Passive microwave sensors can be used to estimate soil moisture but it is hindered by its low spatial resolution. Optical/thermal remote sensing data has become popular in retrieving soil moisture owing to their relatively high spatial, temporal resolution and multiple spectral channels. Since the past decade various methods and indices have been developed to estimate soil moisture. The triangle method and TVDI is one of the most commonly used methods to investigate surface wetness condition owing to the fact that it has a well-defined physical meaning and only requires NDVI and LST to perform the calculation.

TVDI shows, in general, fairly good match in term of the spatial distribution of soil moisture where vegetated areas tend to show low TVDI values indicating high soil moisture, less vegetated and bare soil tend to show high TVDI values meaning low water content. Owing to the fact that the calculation of TVDI is based on the dry edge and the wet edge of a specific date and different date have different driest soil conditions, thus TVDI is not suitable for comparing soil moisture condition across different images. Since wet edges from different images have the same physical meaning (at field capacity or above), so it can be used to derive a more robust surface dryness index. The LST/NDVI feature space consists of a family of soil moisture isolines as well as TVDI isolines, and the slopes of the isolines represent different soil dryness condition, thus the slope of the isolines can be used as an indicator of the soil water content. The Dryness Slope Index (DSI) is proposed based on the wet edge and the slopes of different soil moisture isolines, and it shows a good match in terms of the spatial distribution of soil moisture and a good match for the temporal evolution between soil moisture and the meteorological data.

Evaporative fraction values retrieved from the SEBS model were plotted against DSI, and the regression equations from different plots showed relatively good agreement among each other by using the Willmott index of agreement, which means that there is a uniform

regression function between DSI and evaporative fraction (which is directly related to soil moisture), and in turn it shows that DSI is a more robust surface dryness index than TVDI.

Owing to the limitations of the thermal band from Landsat5 TM data, the LST values estimated are not so continuous that makes the correlation coefficient of EF/DSI plots less satisfying. Some preliminary results from MODIS LST and NDVI products showed higher correlation coefficient, which is assumed to be related to the fact the LST from MODIS data is 12-bit and is more continuous than that of Landsat5 TM data, which is 8-bit. Future studies should be done to see if EF/DSI plots from different dates have similar regression function when using remote sensing data from different sensors and from different study area.

References

Allard M.J.; Meijerink, Carlos R.; Valenzuela and Ann Stewart. 1988 ILWIS: Integrated Land and Watershed Management Information System: Scientific Status Report on the Project, Geo Information System for Land Use Zoning and Watershed Management. Enschede, *The Netherlands: International Institute for Aerospace Survey and Earth Sciences* (ITC).

Carlson, Tobyn.; Gillies, Robertr.; Perry, Eileenm. 1994. A method to make use of thermal infrared temperature and NDVI measurements to infer surface soil water content and fractional vegetation cover. *Remote Sensing Reviews* 9(1): 161-173.

Carlson, Toby N.; Gillies, Robert R.; Schmugge, Thomas J. Carlson, Toby N., 1995; Gillies, Robert R.; Schmugge, Thomas J. *Agricultural and Forest Meteorology*, Vol.77(3), pp.191-205.

Chauhan, N.S., Miller, S., Ardanuy, P., 2003. Spaceborne soil moisture estimation at high resolution: a microwave-optical/IR synergistic approach. *International Journal of Remote Sensing* 24, 4599–4622.

Gao Z.Q, W. Gao, N.B. Chang. 2010. Integrating temperature vegetation dryness index (TVDI) and regional water stress index (RWSI) for drought assessment with the aid of LANDSAT TM/ETM+ images *International Journal of Applied Earth Observation and Geoinformation* 379(10): 1-9.

Gillies, R.R.; Carlson, T.N, 1995. Thermal remote sensing of surface soil water content with partial vegetation cover for incorporation into climate models. *Journal of Applied Meteorology*, Vol.34(4), pp.745-756.

Gillies, R. R.; Kustas, W. P.; Humes, K. S. 1997. A verification of the 'triangle' method for obtaining surface soil water content and energy fluxes from remote measurements of the Normalized Difference Vegetation Index (NDVI) and surface radiant temperature. *International Journal of Remote Sensing* 18, pp. 3145–3166.

Hoeben, R., and Troch, P. A. 2000. Assimilation of active microwave observation data for soil moisture profile estimation. *Water Resour. Res*., 36~10, 2805–2819.

Merlin, O., Al Bitar, A., Walker, J.P., Kerr, Y., 2010. An improved algorithm for disaggregating microwave-derived soil moisture based on red, nearinfrared and thermal-infrared data. *Remote Sensing of Environment* 114, 2305–2316.

Moran, M. S., Clarke, T. R., Inoue, Y., & Vidal, A. 1994. Estimating crop water deficit using the relation between surface-air temperature and spectral vegetation index. *Remote Sensing of Environment,* 49, 246– 263.

Moran, M. S.; Clarke, T.; Kustas, W. P.; Weltz, M.; Amer, S. A. 1994. Evaluation of hydrologic parameters in a semiarid rangeland using remotely sensed spectral data. *Water Resources Research* 30(5): 1287–1297.

Price, J. C. 1990. Using spatial context in satellite data to infer regional scale evapotranspiration. *IEEE Transactions on Geoscience and Remote Sensing*, 28, 940–948.

Prihodko, L.; & Goward, S. N. 1997. Estimation of air temperature from remotely sensed surface observations. *Remote Sensing of Environment* 60 (3), 335 – 346.

Rahimzadeh-Bajgiran P., K., Omasa, Y., Shimizu. 2011. Comparative evaluation of the Vegetation Dryness Index (VDI), the Temperature Vegetation Dryness Index (TVDI) and the improved TVDI (iTVDI) for water stress detection in semi-arid regions of Iran. ISPRS Journal of Photogrammetry and Remote Sensing 68(2012):1-12.

Su, Z 2002. The Surface Energy Balance System (SEBS) for estimation of turbulent heat fluxes. *Hydrology and Earth System Sciences* 6(1): 85-99.

Su, Z. 2001. A Surface Energy Balance System (SEBS) for estimation of turbulent heat fluxes from point to continental scale. In: Su, Z. & C.E. Jacobs (Eds.) Advanced earth observation – land surface climate, final report. pp. 184: Publications of the National Remote Sensing Board (BCRS). USP-2.

Scott, Christopher A.; Bastiaanssen, Wim G. M.; Ahmad, Mobin-Ud-Din. 2003. Mapping Root Zone Soil Moisture Using Remotely Sensed Optical Imagery. *Journal of Irrigation and Drainage Engineering* 129(4): 326-335.

Sandholt, I.; Rasmussen, K.; Andersen, Jens. 2002. A simple interpretation of the surface temperature/vegetation index space for assessment of surface moisture status. *Remote Sensing of Environment* 79, pp. 213–224.

Ulaby, F. T., and Elachi, C., eds. 1990. Radar polarimetry for geoscience applications, Artech House, London.

Verhoest, N. E. C., Troch, P. A., Paniconi, C., and de Troch, F. P. 1998. Mapping basin scale variable source areas from multitemporal remotely sensed observations of soil moisture behavior. *Water Resour. Res*., 34~12, 3235–3244.

Verstraeten, W.W., Veroustraete, F., Feyen, J., 2008. Assessment of evapotranspiration and soil moisture content across different scales of observation. *Sensors* 8, 70–117.

Wang L.L., and J.J. Qu. 2007. NMDI: A normalized multi-band drought index for monitoring soil and vegetation moisture with satellite remote sensing Geophysical research letters 34(20405):1-5.

Willmott C. J.; Wicks D. E. 1980. An empirical method for the spatial interpolation of monthly precipitation within California. *Physical Geography* 1: 59–73.

Xin, J. F., G. L. Tian, Q. H. Liu, and L. F. Chen. 2006. Combining vegetation index and remotely sensed temperature for estimating of soil moisture in China. *International Journal of Remote Sensing* 27(10): 2071-2075.

Zhan Z.M., Q.M. Qin, G. Abduwasit, D.D. Wang. 2007. NIR-red spectral space based new method for soil moisture monitoring. *Science in China Ser D: Earth Sciences* 50(2): 283-289.

Chapter 3 - The Effect of Land Cover and Topography on Simulated Soil Moisture: A Case Study of the Flint Hills Ecoregion and Konza Prairie

Abstract

In this paper, I examined the temporal trend of simulated soil moisture in the Flint Hills ecoregion and then studied the relationships among soil moisture and several environmental factors including land cover, slope, aspect and relative elevation. A series of 16-day MODIS Land Surface Temperature (LST) and Normalized Difference Vegetation Index (NDVI) products from 2000 to 2014 over the entire Flint Hills ecoregion were used to calculate their respective Dryness Slope Index (DSI, Luo *et al,* 2016) images, which were then used to estimate soil moisture in assist of the empirical model which describes the relationship between evaporative faction and soil moisture. I then used the nonparametric Mann-Kendall (MK) test on the simulated soil moisture to explore whether any trend is present throughout the years. Results showed that there is no statistically significant upward or downward trend found in the dataset. The Univariate Analysis of Variance (ANOVA) test was conducted to explore the effect of land cover and some topographic factors on simulated soil moisture, and results showed that land cover contributes the most to the variations of simulated soil moisture.

Key words: TVDI, dryness slope index (DSI), soil moisture, temporal trend, relative importance.

Introduction

Soil moisture is an important variable for hydrological processes, energy exchange and land-atmospheric interactions. It serves as an essential index for drought prediction and has great implications for agricultural activities and management. Soil moisture dynamics are controlled by many processes including evapotranspiration, infiltration and root water uptake. Soil moisture is also a vital factor which determines the spatial and temporal dynamics of terrestrial ecosystems and is therefore a key variable in ecological and hydrological models, and the retrieval of soil moisture at regional and global scale has become the focus of many studies of land surface processes (Moran *et al*., 1994).

Field investigation is one the most commonly used methods for retrieving soil and vegetation water content. Even though it provides the most accurate information about soil moisture, this method is not suitable to be applied to remote and mountainous areas as it is costly and time-consuming which also limited its spatial coverage and investigation frequency. What is more, point-based data is often poorly-distributed and are not available in a timely manner. For this reason, the use of remote sensing to retrieve soil moisture has become the focus of many studies (Carlson *et al*., 1995a; Gillies and Carlson, 1995b; Verstraeten *et al*., 2008) despite the difficulty of obtaining reliable estimates. Since soil moisture has important implications in regional resources and environments, and land use/cover and other related environmental factors influence the spatial distribution and temporal evolution of soil moisture, understanding the spatial and temporal relationships between soil moisture and these factors is of great significance for more efficient and sustainable use of the available soil moisture and other resources.

Optical and thermal radiation and reflection characteristics are largely controlled by the soil and vegetation. Vegetation has a unique spectral response, which has high reflectance at near-infrared wavelength and low reflectance at red wavelength (Figure 3.1). This is largely controlled by the chlorophyll content in the leaves, which in turn can be influenced by soil water content. Therefore, the soil water content can be indirectly reflected by the spectral response, and the Normalized Difference Vegetation Index (NDVI) is the most common used index to reveal vegetation health condition. Soil moisture also influences the reflectance of the soil because soil reflectance decreases with increasing soil water content. Soil moisture can also influence the temperature of the soil surface and the canopy.

Although, the spectral reflectance of the canopy does not change greatly after initial water stress, the temperature of the leaves can rise rapidly. The temperature of the soil is closely related to sensible heat and latent heat which is largely controlled by the soil water content. Therefore, a variety of methods which utilize remote sensing to estimate soil water content are based on Land Surface Temperature (LST), Normalized Difference Vegetation Index (NDVI), and other related indices. Wang *et al.,* (2007) used three channels from MODIS data, centering at 860 nm, 1640 nm and 2130 nm, and proposed the Normalized Multi-Band Drought Index (NMDI) to estimate soil moisture. Zhan *et al*., (2007) proposed the model of Soil Moisture Monitoring by Remote Sensing (SMMRS) based on the near-infrared versus red spectral reflectance feature space from which evaporative fraction is derived, and SMMRS is calculated by subtracting evaporative fraction from 1 which represents the soil moisture of a completely wet soil. Among many different surface dryness indices, the triangle method and the notion of temperature vegetation dryness index have attracted the most attention (Price, 1990, Carlson *et al*., 1994). The "triangle" method utilizes the feature space of LST versus NDVI to represent physical boundaries of the surface, therefore bypasses the need for additional atmospheric data to estimate soil water content. Owing to the fact that the calculation of TVDI depends on the "wet edge" and the "dry edge" position whose physical meaning, the driest condition of the frame, varies among different images from different date. Whereas, the "wet edge" has a fairly stable physical meaning which is at field capacity or above. Therefore, in this study we adopted a modified form of TVDI, the Dryness Slope Index (DSI, Luo *et al*, 2016), to estimate soil water content. Then, we explored the temporal evolution of soil moisture in Flint Hills from 2000 to 2014 to verify whether there is an upward or downward trend throughout the years. In order to understand the relationships among soil moisture and several environmental variables, a one-way ANOVA was applied to see which environmental factor contribute the most the variations of soil moisture.

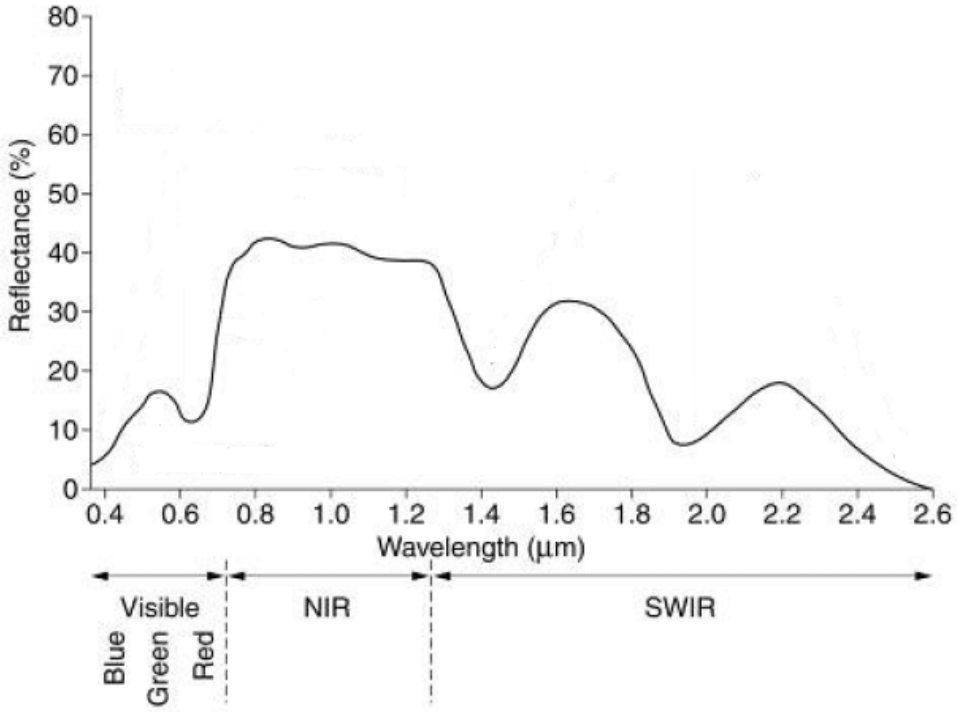

Figure 3.1 Green vegetation spectral curve. At the red wavelength it shows low reflectance, and at NIR it shows high reflectance. Modified from source: Assessing the Extent and Severity of Erosion on the Upland Organic Soils of Scotland using Earth Observation: A GIFTSS Implementation Test: Final Report. October 2009.

Study area and dataset

The study area includes the Flint Hills ecoregion, an area of 25,733km^2, is located in eastern Kansas and north-central Oklahoma (See Figure 3.1). The main land cover of the Flint Hills ecoregion includes dense grassland, shrub, open water, developed areas, and cropland along the river valleys and in areas with little relief. Average annual precipitation ranges from 711 mm to 889 mm. The main soil types include Kastanozems (Dark brown soils rich in organic matter) and Phaeozems (Dark soils rich in organic matter). The study area also includes the Konza Prairie Biological Station (KPBS). KPBS is a 73 km^2 study area is located south of Manhattan, Kansas. It is a member of the National Science Foundation's Long Term Ecological Research (LTER) network, and thus maintains an extensive archive of ecological and climatological data supporting this research. The site includes the entire Konza prairie and some agricultural land in the north of the Konza prairie. The main land cover is grassland, woodland, cultivated crops, barren land and open water. Except for agricultural lands whose land cover type varies throughout a year, other land cover types remain relatively stable. Around 76% of annual rainfall (835 mm) occurs during the growing season, and it is highly variable from year to year. The main soil types in the study area are silt loam and silty clay loam.

The dataset comes from several sources. The MODIS LST (MOD11A2) and NDVI (MOD13A2) products (NASA LP DAAC, 2000) from May to October from 2000 to 2014 with an interval of 16 days are utilized to calculate soil moisture and to explore its temporal change for the Flint Hills ecoregion. Land cover map (obtained from classifying Landsat5 TM images) and topography data (DEM) are used to explore their relative importance to the variations of estimated soil moisture.

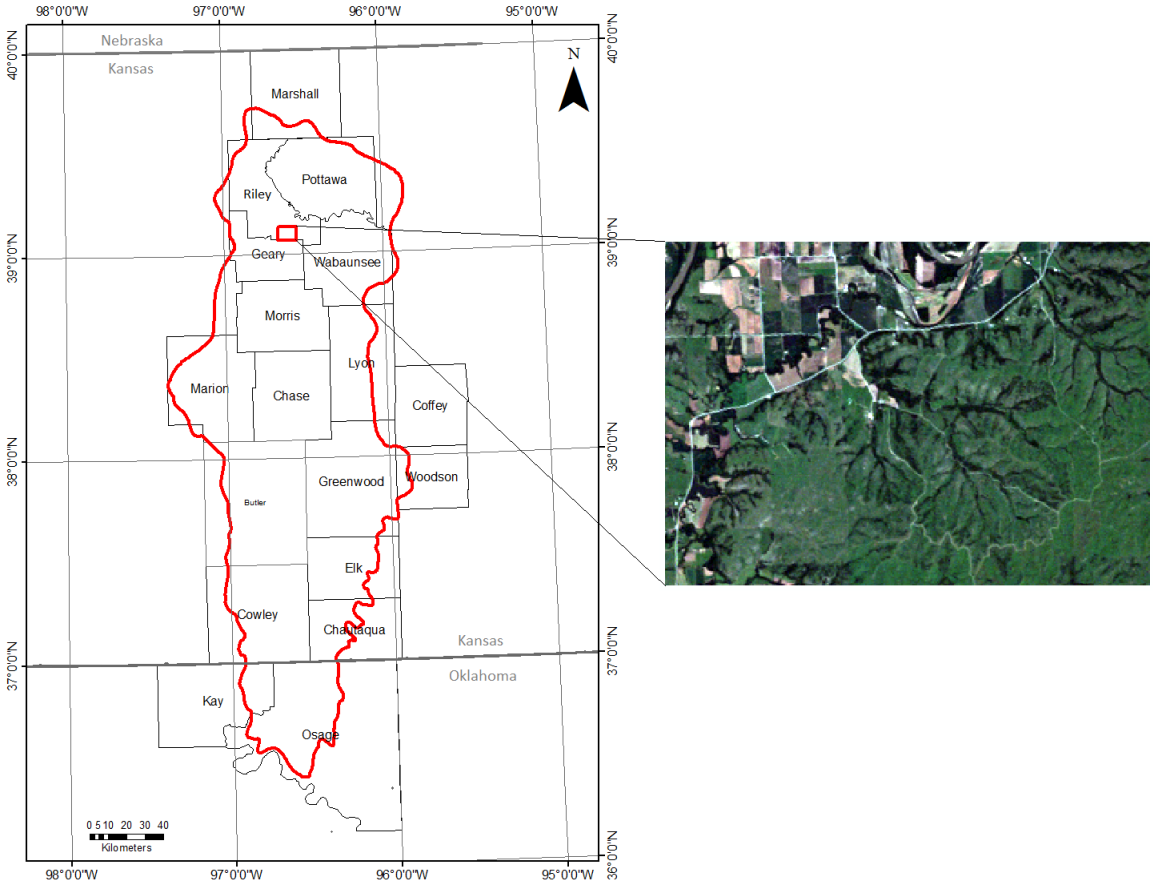

Figure 3.2 Two study area (marked by red boundaries)

Method

The "triangle" method and its modified form----the dryness slope index

The "triangle" method is based on an interpretation of the pixel distribution in LST/NDVI feature space. LST is affected by several factors including surface thermal properties, evapotranspiration, and vegetation coverage, hence there is no direct relationship between LST and soil water content. However, soil moisture is an important factor controlling vegetation canopy temperature. Studies show that under certain vegetation coverage soil moisture can indirectly affect canopy temperature. Usually the LST/NDVI feature space (shown in Figure 3.3) is used to illustrate the relationship among LST, soil moisture and vegetation coverage. A scatterplot of remotely sensed surface temperature and a vegetation index often results in a triangular shape (Price, 1990; Carlson *et al*., 1994), or a trapezoid shape (Moran, Clarke, Inoue, *et al.*, 1994) if a full range of fractional vegetation cover and soil moisture contents is represented in the data. Many studies (Prihodko and Goward 1997; Moran *et al*. 1994; Carlson et al. 1995; Gillies *et al.* 1997; Sandholt *et al.* 2002) show that the "triangle" shape can be regarded as consisting of a family of soil moisture isolines representing different degrees of aridity. The horizontal line at low limit in the LST/NDVI feature space is called the wet edge (unlimited water availability) while the sloping line is called the dry edge (maximum evapotranspiration and limited water access). A dryness index is proposed from the LST/NDVI feature space to describe the relationship among the three and it is calculated as the ratio of A to B for point C in the feature space:

$$TVDI = \frac{T_c - T_{min}}{T_{max} - T_{min}} = \frac{A}{B} \qquad (1)$$

where T_c represents the LST of a pixel; T_{min} is the temperature at the wet edge; T_{max} represents the temperature at the dry edge under the same NDVI and is calculated as T_{max} = a + b*NDVI, where a and b are the coefficients of the regression equation for the dry edge. As how the index is defined above, the TVDI value at dry edge would be 1 and that at the wet edge is 0.

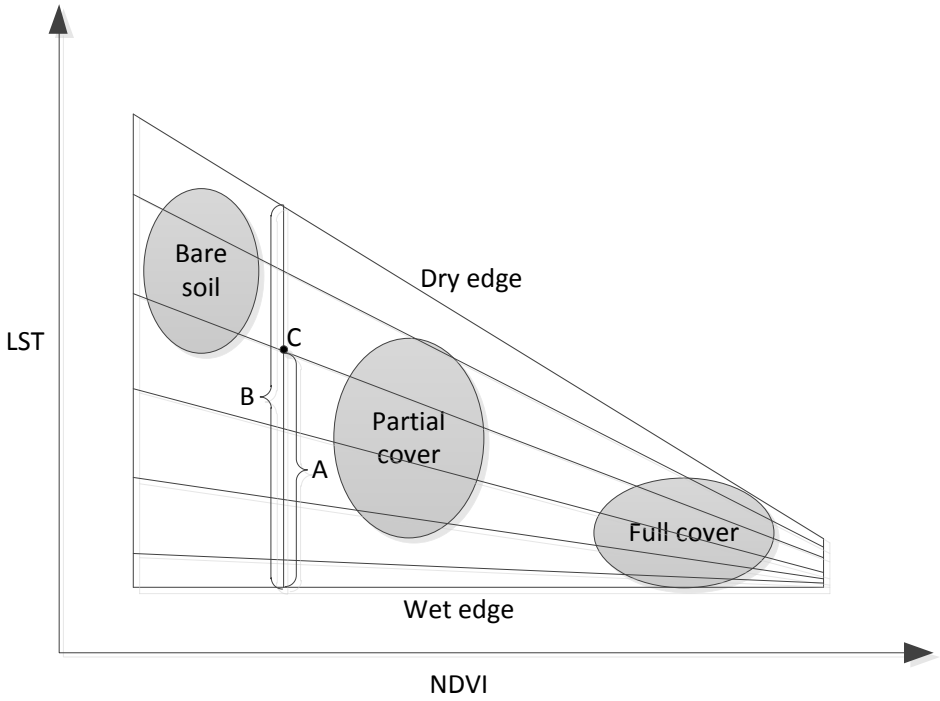

Figure 3.3 LST/NDVI Feature Space. Bare soil pixels tend to exist in the upper-left corner of the triangle; Full vegetation pixels appear in the bottom-right corner of the triangle; Mixed pixels appear in the center of the feature space. For pixel C, its TVDI value calculates as the ratio between A (the distance from its LST value to the wet edge) and B (the distance between the maximum LST under the same NDVI to the wet edge). The slanting lines within the LST/NDVI feature space are TVDI isolines.

From the above analysis, it is apparent that TVDI is based on the dry edge as well as the wet edge. The former varies for different dates and different feature spaces, whereas the latter has a fairly stable physical meaning behind it which is at field capacity or above. Recall that the LST/NDVI feature space consists of a family of soil moisture isolines which are also TVDI isolines, and drier soil has steeper isolines whereas wetter one has moderate isolines. The slope is confined in the specific feature space and its maximum value is no greater than the slope (its absolute value) of the dry edge of the same frame. We can then use the slope of soil moisture isolines as a measurement to show how far each soil moisture isoline is deviated from the wet edge, thus we have the same basis for different images. From the above analysis DSI is defined as the slope (its absolute value) of each soil moisture isoline, and the formulation of this index is calculated as (Luo *et al*. 2016):

$$DSI = |a * TVDI| \quad (2)$$

where *a* is the slope of the dry edge for a specific frame; TVDI is the TVDI value for each pixel within the frame. Since the slope of the dry edge is negative, the absolute value is used to show how far a soil moisture isoline is deviated from the wet edge. As a result, drier pixel would be further from the wet edge and thus has larger DSI values.

An empirical model between DSI and evaporative fraction

Luo *et al*. (2016) proposed an empirical linear model which describes the relationship between DSI and evaporative fraction (EF). It is calculated as:

$$EF = -0.0422 * DSI + 1.1179 \quad (3)$$

An empirical model between soil moisture and evaporative fraction

Scott *et al.* (2003) proposed a way to estimate relative soil moisture based on evaporative fraction:

$$\theta = \theta_{sat} * e^{(\Lambda-1)/0.42} \quad (4)$$

where θ_{sat} is the saturated soil moisture, Λ is the evaporative fraction.

According to equation 2,3,4, soil moisture can be expressed as:

$$\theta = \theta_{sat} * e^{(-0.0422*|a*TVDI|+0.1179)/0.42} \quad (5)$$

Temporal analysis of soil moisture

Mann and others (e.g. Mann 1945; Kendall 1975; Gilbert 1987) proposed using the test for significance of Kendall's tau (MK test) to statistically assess if there is a monotonic upward or downward trend of the variable of interest over time. The MK test is a nonparametric test which means it does not require the assumption of normality. The null hypothesis is that there is no trend and the alternative hypothesis is that there is a trend (upward or downward) in the dataset. The Kendall's tau-b test is calculated as follows and statistic software SPSS is used to calculate the tau-b value:

$$\tau_B = \frac{n_c - n_d}{\sqrt{(n_0 - n_1)(n_0 - n_2)}} \quad (6)$$

where:

n_c is the number of concordant pairs;

n_d is the number of concordant pairs;

n_0 equals $n(n-1)/2$;

n_1 equals $\sum_i t_i(t_i - 1)/2$;

n_2 equals $\sum_j u_j(u_j - 1)/2$;

t_i is the number of tied values in the i^{th} group of ties for the first quantity;

u_j is the number of tied values in the j^{th} group of ties for the second quantity;

MODIS NDVI and LST products were processed to calculate soil moisture values by using equation 5. The nonparametric MK test was applied on the mean value of estimated soil moisture of the entire Flint Hills eco-region, and three land cover types, namely, forest, grassland, and cultivated crop land.

Relationship among simulated soil moisture and land cover and topography

In order to explore the relationship among simulated soil moisture and several environmental factors including land cover, slope, aspect and relative elevation, a one-way ANOVA test was used. Land cover maps were produced for day 2008205, 2008173, and 2008221 by using Landsat5 TM images for these days. Topographic factors were extracted from 30-m spatial resolution DEM. Then, around 2,500 (5% of all pixels) pixels are randomly selected to perform ANOVA test to explore the relative importance of those environmental factors to soil moisture variations. The null hypothesis of ANOVA test is that the mean of simulated soil moisture is the same for different groups within each environmental factor. The alternative hypothesis is that the means for each group are not equal.

Results

Temporal analysis

Average soil moisture values for Flint Hills ecoregion from 134 different dates were calculated and then MK test was used to verify if there is a statistically significant upward or downward trend existing in the dataset. Plots of average soil moisture values for the entire Flint Hills ecoregion and its forest, grassland, and cultivated crop land of these different dates are shown below (See Figure 3.4, Figure 3.5, and Figure 3.6). The general trend of simulated soil moisture within a certain year is that it gradually goes down and reaches the lowest point around the middle of the year, and then it slowly rises. The result of MK test is shown in Table 3.1, and an example of estimated soil moisture for the entire Flint Hills Ecoregion is also shown (See Figure 3.7; using image from July 28th 2010).

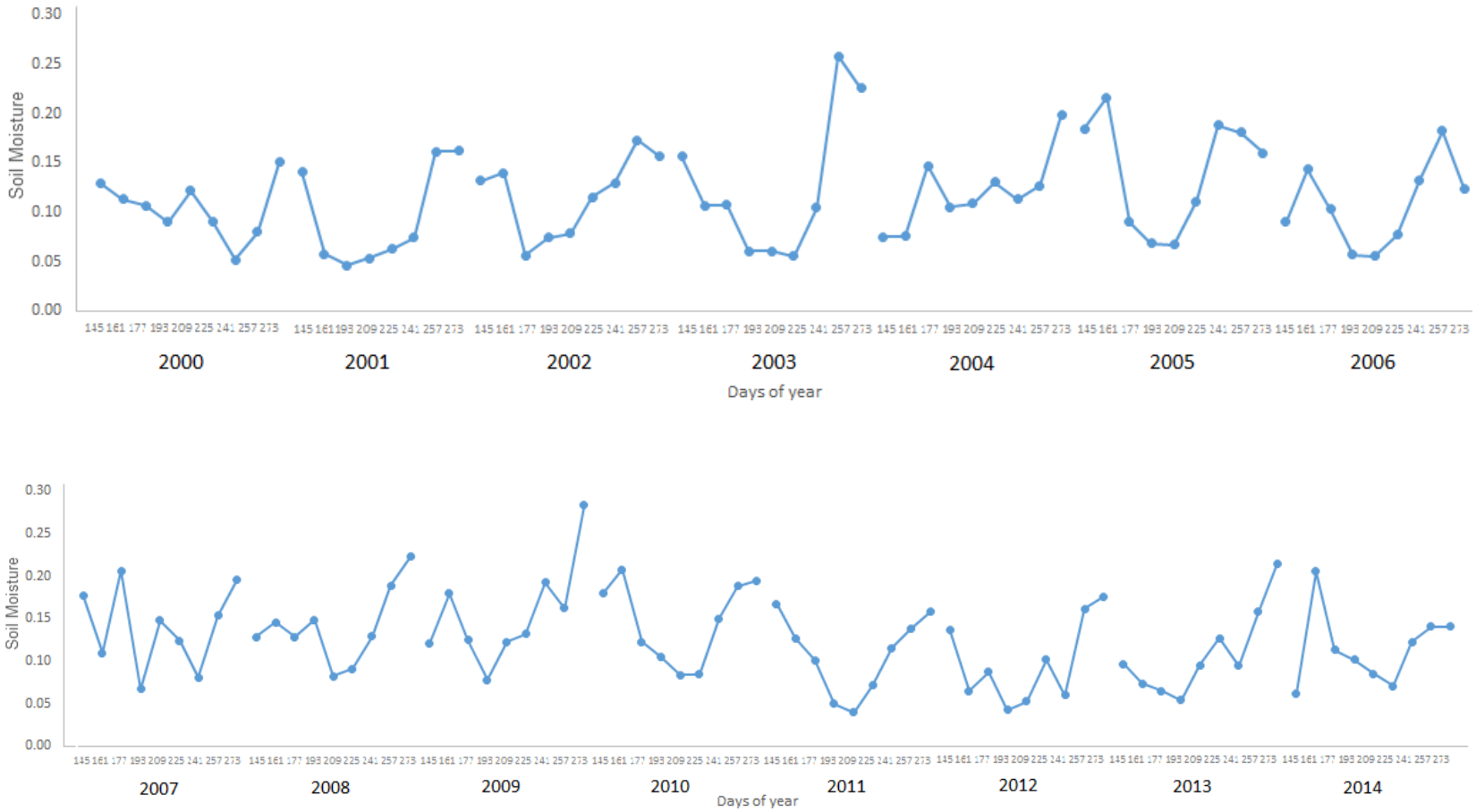

Figure 3.4 Plots of mean soil moisture values for the entire Flint Hills Ecoregion throughout the years. The general trend of simulated soil moisture within a certain year is that it gradually goes down and reaches the lowest point around the middle of the year, and then it slowly rises.

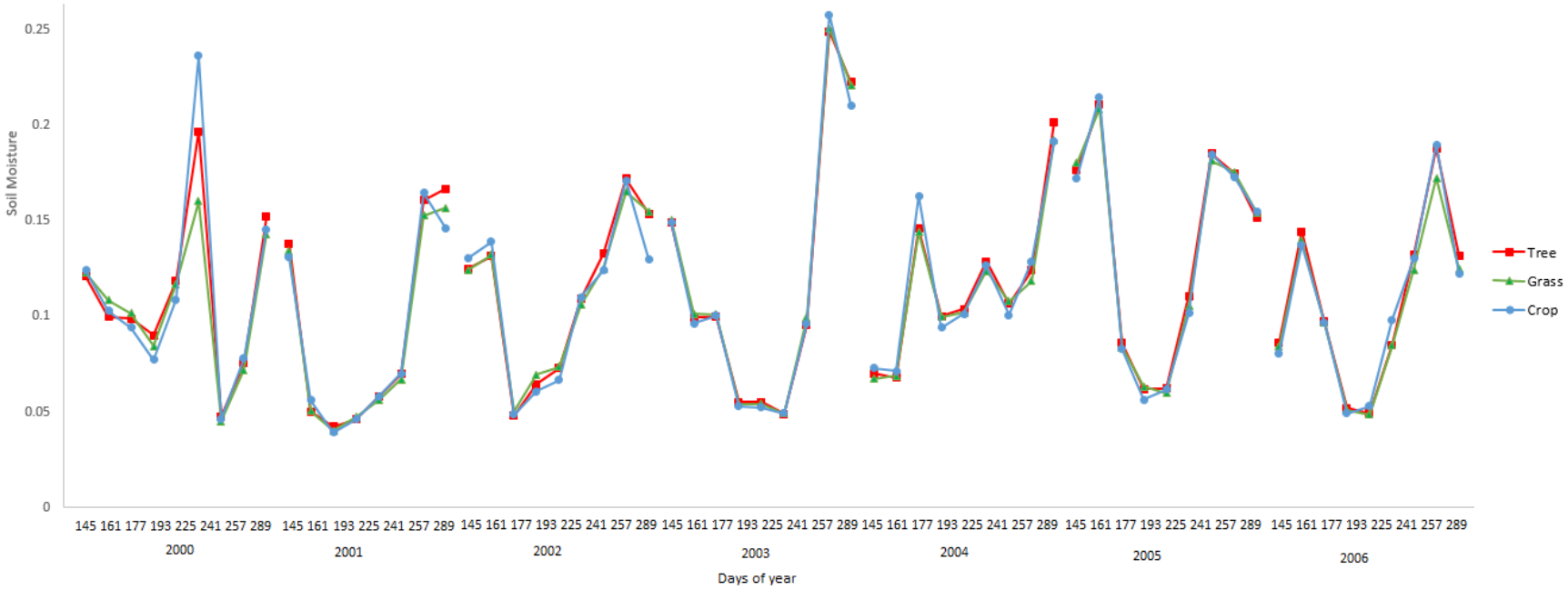

Figure 3.5 Plots of mean soil moisture values for three different land cover types from 2000 to 2006

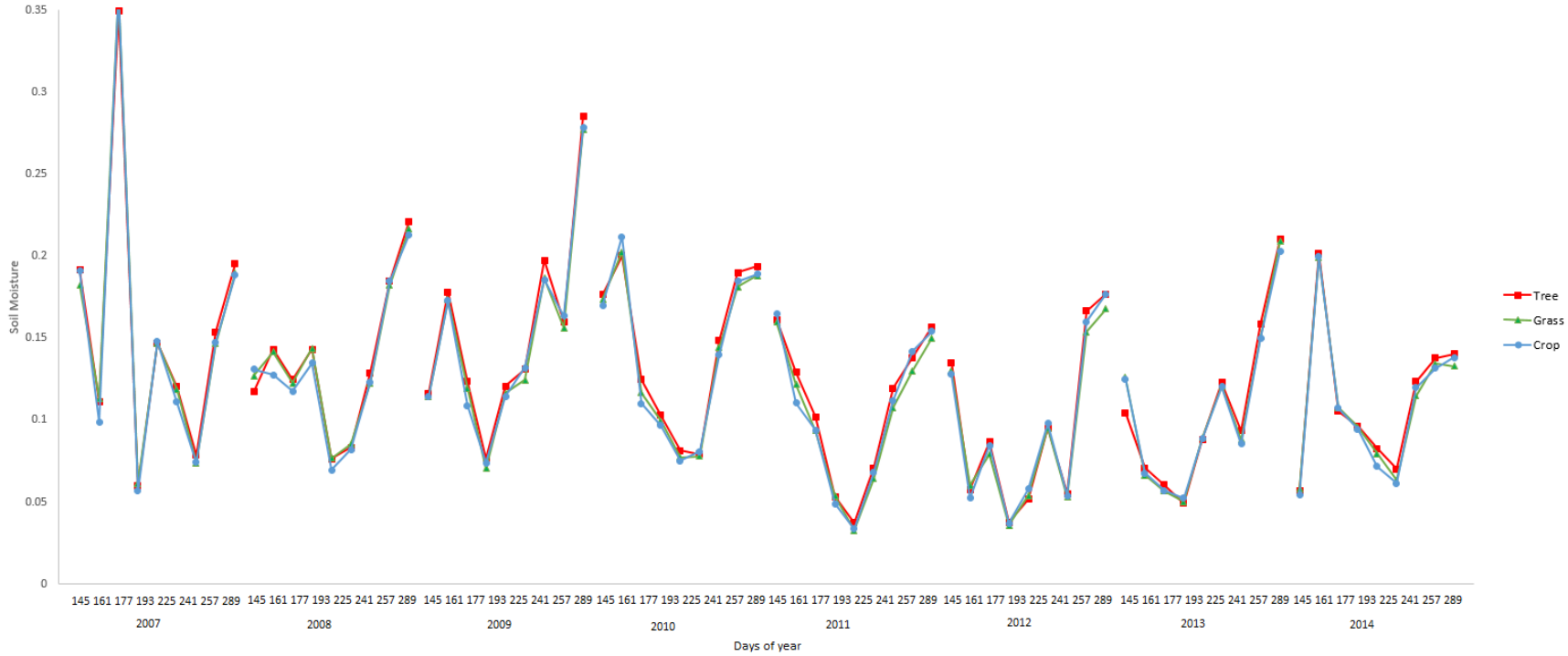

Figure 3.6 Plots of mean soil moisture values for three different land cover types from 2000 to 2014

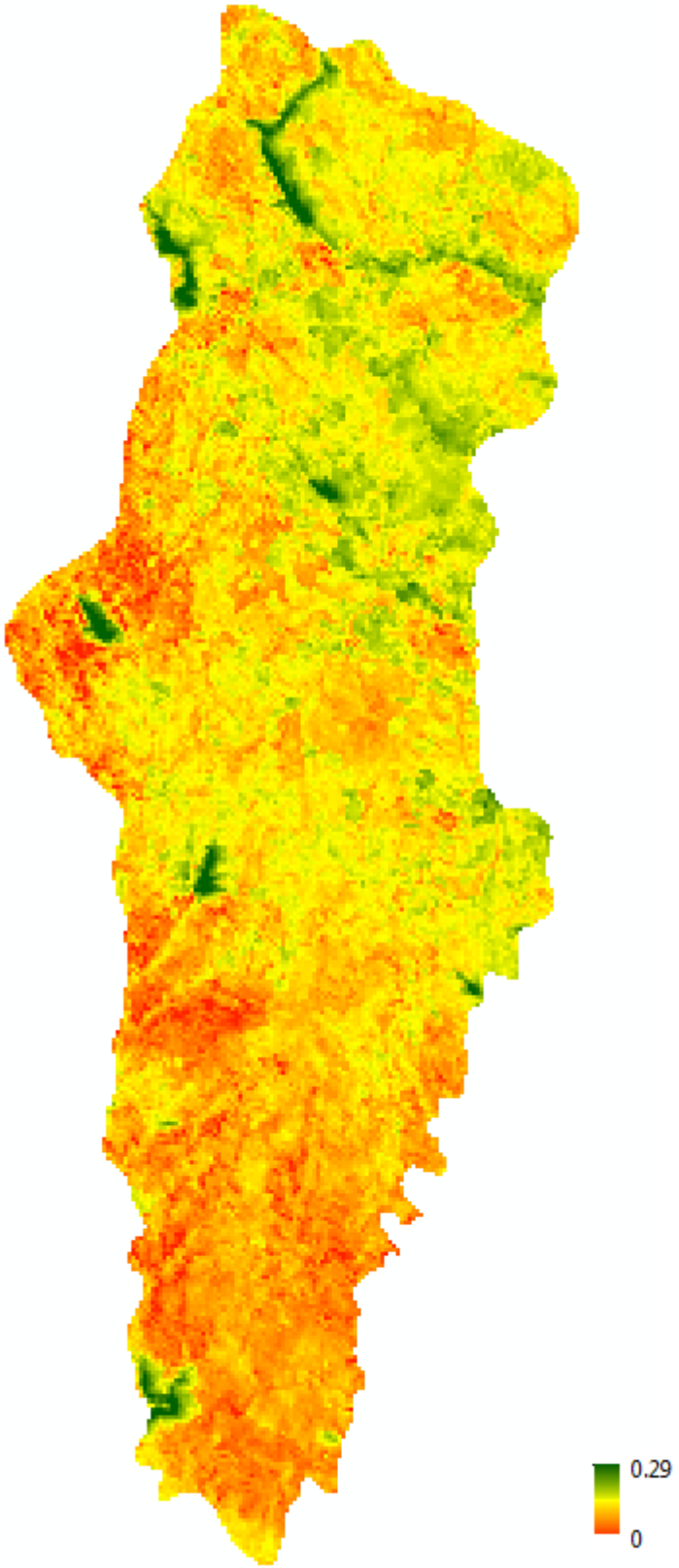

Figure 3.7 Simulated soil moisture for the Flint Hills Ecoregion from July 28th, 2010

Table 3.1 MK result for trend analysis

	Tau	P value	Alpha
Flint Hills ecoregion	-0.038	0.519	0.05
Forest	0.039	0.501	0.05
Grassland	0.031	0.593	0.05
Cultivated crop land	0.032	0.580	0.05

The low tau value between time and estimated soil moisture suggests that there is little correlation between them. The p value is larger than the significance level alpha meaning that the null hypothesis is not rejected, so there is no significant trend in soil moisture values for the Flint Hills ecoregion and the three land cover types over the years. However, this conclusion comes from using MODIS product whose spatial resolution is 1 km and from looking at the entire Flint Hills ecoregion for a certain period of time. Therefore, an upward or downward may show up if using a finer spatial resolution data or a smaller study area at a different time.

The relationships among soil moisture and land cover and topographic factors

The result of ANOVA test is shown in the Table 3.2. As we can see that for 2008205 and 2008221 land cover, aspect, and relative elevation have significant effects on the variability of soil moisture values to which, however, slope contributes little. Result from 2008125 shows that only land cover is statistically significantly related to the soil moisture variations. Land cover has larger F value than other factors indicating a greater possibility that it accounts for most of variability in simulated soil moisture. Since the calculation of simulated soil moisture is based on DSI, which is related to NDVI and LST, so it is understandable that land cover shows direct and larger impact on soil moisture variations. However, soil moisture estimated by using a hydrology model, which considers elevation factors may show a different result where slope and other topographic factors have more influence than land cover on the variations of estimated soil moisture.

Table 3.2 ANOVA results

	2008125			2008205			2008221		
Factors	F	Critical F value	*p*	F	Critical F value	*p*	F	Critical F value	*p*
Land cover	5.91	2.99	0.03	32.11	2.99	0.00	6.89	2.99	0.001
Aspect	0.85	1.88	0.56	1.91	1.88	0.04	2.59	1.88	0.005
Relative elevation	1.07	1.219	0.28	2.63	1.21	0.00	2.25	1.21	0.000
Slope	0.97	1.12	0.62	0.83	1.12	0.98	1.05	1.09	0.110

Discussion and Conclusion

Soil moisture is an important biophysical property of soil which controls evapotranspiration, energy exchange, and vegetation coverage on the surface. It is also an important factor for monitoring drought and has many implications for agricultural managements. Monitoring soil moisture at regional and continental scales over a long period can provide insights for environmental evaluation and protection, and it has been difficult to achieve via traditional methods, such as field investigation. Remote sensing has provided an alternative to observe the surface at a much larger scale and at a timely manner, which makes it more plausible to monitor soil moisture at a large scale. The means of remote sensing has become popular in spite of inaccuracy compared to field investigation. Since anthropogenic activities can change land use and cover which in turn changes the spatial and temporal distribution of soil moisture, understanding the relationships among soil moisture, land cover, and topography is beneficial to efficient use of the available soil moisture and other resources.

In this study, I estimated soil moisture over the entire Flint Hills ecoregion from 2000 to 2014 by using a form of modification of the temperature vegetation dryness index, called dryness slope index in assist of several empirical models which illustrate the relationship between soil moisture and evaporative fraction. I then applied the nonparametric Mann-Kendall test to verify if any trend was present in soil moisture over the years, and the results showed that there is no statistically significant relationship between soil moisture and time and no upward or downward trend was found in the dataset. This indicates that soil water content has not seen major changes over the entire Flint Hills ecoregion from 2000 to 2014. However, this result could be different when using a different dataset or different study area. We then focused on a smaller study area (Konza Prairie and its nearby areas) to explore the relationship among simulated soil moisture, land cover, and topography. The univariate analysis of variance was conducted for about 2,500 randomly selected pixels, and the results showed that land cover has the biggest influence on soil moisture than slope, aspect, and relative elevation. This is likely owing to the fact that the dryness slope index is based on TVDI whose calculation depends on NDVI and land surface temperature; therefore it is reasonable and understandable that land cover contributes the most to the variations of estimated soil moisture. In this study, we did not attempt to compare soil

moisture from field investigation and its relationships to the environmental factors, so further studies should be carried out to see if soil moisture from field data could give similar results.

References

Carlson, Tobyn.; Gillies, Robertr.; Perry, Eileenm. 1994. A method to make use of thermal infrared temperature and NDVI measurements to infer surface soil water content and fractional vegetation cover. *Remote Sensing Reviews* 9(1): 161-173.

Carlson, Toby N.; Gillies, Robert R.; Schmugge, Thomas J. Carlson, Toby N., 1995; Gillies, Robert R.; Schmugge, Thomas J. *Agricultural and Forest Meteorology*, Vol.77(3), pp.191-205.

Gilbert, R.O. 1987. Statistical Methods for Environmental Pollution Monitoring, Wiley, NY.

Gillies, R.R.; Carlson, T.N, 1995. Thermal remote sensing of surface soil water content with partial vegetation cover for incorporation into climate models. *Journal of Applied Meteorology*, Vol.34(4), pp.745-756.

Gillies, R. R.; Kustas, W. P.; Humes, K. S. 1997. A verification of the 'triangle' method for obtaining surface soil water content and energy fluxes from remote measurements of the Normalized Difference Vegetation Index (NDVI) and surface radiant temperature. *International Journal of Remote Sensing* 18, pp. 3145–3166.

Kendall, M.G. 1975. Rank Correlation Methods, 4th edition, Charles Griffin, London.

Luo, L., Goodin, G. G., Wang, J. 2016. The Dryness Slope Index (DSI) – A Modified Form of the Temperature Vegetation Dryness Index (TVDI) for Estimating Soil Moisture. *Publication* i*n Preparation*.

Mann, H.B. 1945. Non-parametric tests against trend, *Econometrica* 13(3):245-259.

Moran, M. S., Clarke, T. R., Inoue, Y., & Vidal, A. 1994. Estimating crop water deficit using the relation between surface-air temperature and spectral vegetation index. *Remote Sensing of Environment*, 49, 246– 263.

Moran, M. S.; Clarke, T.; Kustas, W. P.; Weltz, M.; Amer, S. A. 1994. Evaluation of hydrologic parameters in a semiarid rangeland using remotely sensed spectral data. *Water Resources Research* 30(5): 1287–1297.

NASA LP DAAC, 2000, The level-3 MODIS global Land Surface Temperature (LST) and Emissivity 8-day. NASA EOSDIS Land Processes DAAC, USGS Earth Resources Observation and Science (EROS) Center, Sioux Falls, South Dakota (https://lpdaac.usgs.gov), accessed July 1, 2015, at https://lpdaac.usgs.gov/dataset_discovery/modis/modis_products_table/mod11a2.

NASA LP DAAC, 2000, The level-3 MODIS global Vegetation Indices 16-Day L3 Global 1km. NASA EOSDIS Land Processes DAAC, USGS Earth Resources

Observation and Science (EROS) Center, Sioux Falls, South Dakota (https://lpdaac.usgs.gov), accessed July 1, 2015, at https://lpdaac.usgs.gov/dataset_discovery/modis/modis_products_table/mod13a2.

Price, J. C. 1990. Using spatial context in satellite data to infer regional scale evapotranspiration. *IEEE Transactions on Geoscience and Remote Sensing*, 28, 940–948.

Prihodko, L.; & Goward, S. N. 1997. Estimation of air temperature from remotely sensed surface observations. *Remote Sensing of Environment* 60 (3), 335 – 346.

Sandholt, I.; Rasmussen, K.; Andersen, Jens. 2002. A simple interpretation of the surface temperature/vegetation index space for assessment of surface moisture status. *Remote Sensing of Environment* 79, pp. 213–224.

Scott, Christopher A.; Bastiaanssen, Wim G. M.; Ahmad, Mobin-Ud-Din. 2003. Mapping Root Zone Soil Moisture Using Remotely Sensed Optical Imagery. *Journal of Irrigation and Drainage Engineering* 129(4): 326-335.

Verstraeten, W.W., Veroustraete, F., Feyen, J., 2008. Assessment of evapotranspiration and soil moisture content across different scales of observation. *Sensors* 8, 70–117.

Wang L.L., and J.J. Qu. 2007. NMDI: A normalized multi-band drought index for monitoring soil and vegetation moisture with satellite remote sensing Geophysical research letters 34(20405):1-5.

Zhan Z.M., Q.M. Qin, G. Abduwasit, D.D. Wang. 2007. NIR-red spectral space based new method for soil moisture monitoring. *Science in China Ser D: Earth Sciences* 50(2): 283-289.

Chapter 4 – Conclusions

Optical/thermal remote sensing is one of the most commonly used methods to retrieve soil water information, and there are many surface dryness indices being proposed for that purpose. Throughout the years, the triangle method and TVDI have been developed and adopted to estimate soil moisture from local to global scale. However, little attention has been paid to the theoretical basis of the triangle method. In this thesis, I examined the theoretical basis of the calculation of TVDI and proposed a more robust dryness index based on TVDI. The new surface dryness index was then applied to study the temporal trend of soil moisture over the entire Flint Hills ecoregion. I used a small study area, which is mainly located in the Konza prairie, to study the relationships among soil moisture and several environmental variables.

Chapter 2, The Dryness Slope Index (DSI) – A Modified Form of the Temperature Vegetation Dryness Index (TVDI) for Estimating Soil Moisture, carefully examined the theoretical basis of the triangle method by using the surface energy balance system model (SEBS). Several assumptions about the triangle method were verified, including (1) the LST/NDVI feature space would result in a triangular shape given enough pixels reflecting a full range of soil surface wetness and vegetation coverage; (2) The LST/NDVI feature space consists of a family of soil moisture isolines which are also TVDI isolines, and more slanting isolines correspond to drier soil pixels, and vice versa ; (3) The upper boundary of the LST/NDVI feature space represents the driest condition in the specific frame and the lower boundary represents soil with unlimited water availability. The calculation of TVDI is based on the position of the dry edge and the wet edge, and the former of which represents the driest condition of the frame and the later stands for soil pixel at field capacity or above. The driest condition does not necessarily mean zero soil moisture, and driest condition from different frames may vary. Therefore, TVDI value calculated from different image cannot be used as an indicator as to say one pixel from one image is drier than the pixel from another image. On the other hand, the wet edge has a stable physical meaning even among different images, and it can be utilized to develop a more robust dryness index whose value can be compared among different images. With the help soil moisture isolines, a new dryness index, the Surface Dryness Index (DSI), which reflects how far each soil moisture isoline is deviated from the wet edge, was proposed. In order to

show the performance of TVDI and DSI in estimating soil moisture, spatial distribution and temporal evolution of soil moisture estimated from TVDI and DSI were compared, and results showed that the spatial pattern of soil moisture from these two indices are similar. However, temporal evolution of soil moisture calculated from TVDI showed some abnormality with the precipitation data. Dates which received significant rainfall showed higher TVDI values than those received little rainfall. However, the temporal change of soil moisture from DSI showed a more reasonable match with the rainfall record. In order to show that there is a uniform relationship between DSI and evaporative fraction, four different images were chosen to perform the Willmott index of agreement test. Results showed that an uniform relationship was found between DSI and evaporative fraction among different images. To take it further, an empirical model about DSI and soil moisture was developed in the end.

Chapter 3, The Effect of Land Cover and Topography on Simulated Soil Moisture: A Case Study of the Flint Hills Ecoregion and Konza Prairie, applied the new index ---- DSI developed in chapter 2 to study temporal trend of soil moisture and its relationships with several environmental variables. A series of 16-day MODIS Land Surface Temperature (LST) and Normalized Difference Vegetation Index (NDVI) products from 2000 to 2014 over the entire Flint Hills ecoregion were used to calculate their respective temperature DSI images which were then utilized to estimate soil moisture in assist of the empirical model which describes the relationship between evaporative faction and soil moisture. The nonparametric Mann-Kendall (MK) test was then used on the simulated soil moisture to explore whether any trend is present throughout the years. Results showed that little correlation was found in soil moisture over time and there was no upward or downward trend throughout the years. In order to address how anthropogenic activities, such as land use/cover change, affect spatial distribution of soil moisture, another study was carried out in a smaller study area mainly located at the Konza Prairie. Four environmental variables, including land cover, slope, aspect, and relative elevation, from three different dates were extracted along with their corresponding soil moisture images. A one-way ANOVA test was then used on soil moisture and the environmental variables. Results showed that land cover has larger F value than other factors indicating a greater possibility that land cover accounts for most of variability in simulated soil moisture. This is likely owing to the fact

that DSI is based on TVDI whose calculation depends on NDVI and LST; therefore, it is reasonable and understandable that land cover contributes the most to the variations of estimated soil moisture.

Appendix

Triangle_main.py

```
import os
from triangle import Indices
import auxil.auxil as auxil
import gc
def main():
#   input directory
    in_path = auxil.select_directory(title="Choosing the input file directory")
#   imagery dataset
    lista = os.listdir(in_path)
    print in_path
    GQ = []
    data_list=[]
    i = 0
    for k in range(len(lista)):
        GQ.append(str(lista[k]))
    for k in GQ:
        try:
            if float(k[16:23]) > 0 :
                data_list.append(k[16:23])
        except StandardError, e:
            print "Error!"
```

```
    print data_list[0:len(data_list)/2]
#   Output txt
    Count = len(data_list)/2
    for m in data_list[0:len(data_list)/2]:
        print m
        print type(m)
        Indices(in_path, m, Count)
    print m
```

Triangle.py

```
    import auxil.auxil as auxil
    import numpy as np
    from osgeo import gdal
    from osgeo.gdalconst import GA_ReadOnly,GDT_Float32
    import matplotlib.pyplot as plt
    from pylab import *
    import gc

    def Indices(in_path,M, Count):
    #   Input NDVI file
        print "***************"
        print str(M)
```

```
    gdal.AllRegister()
    band_NDVI =
gdal.Open(in_path+"/MOD13A2.MRTWEB.A"+M+".005.1_km_16_days_NDVI.tif",G
A_ReadOnly)
    try:
        cols1 = band_NDVI.RasterXSize
        rows1 = band_NDVI.RasterYSize
        bands1 = band_NDVI.RasterCount
    except StandardError, e:
        print "Error: "+str(M)+"_NDVI is missing"
        exit(1)
  #   Input LST file
    if(1):
        band_LST =
gdal.Open(in_path+"/MOD11A2.MRTWEB.A"+M+".005.LST_Day_1km.tif",GA_Read
Only)
    if(band_LST is None):
        band_LST =
gdal.Open(in_path+"/MOD11A2.MRTWEB.A"+M+".041.LST_Day_1km.tif",GA_Read
Only)
    if(band_LST is None):
        band_LST =
gdal.Open(in_path+"/MOD11A2.MRTWEB.A"+M+".004.LST_Day_1km.tif",GA_Read
Only)
    if(band_LST is None):
```

```
        band_LST =
gdal.Open(in_path+"/MOD11A2.MRTWEB.A"+M+".005.LST_Day_1km.tiff",GA_Rea
dOnly)
    if(band_LST is None):
        band_LST =
gdal.Open(in_path+"/MOD11A2.MRTWEB.A"+M+".041.LST_Day_1km.tiff",GA_Rea
dOnly)
    if(band_LST is None):
        band_LST =
gdal.Open(in_path+"/MOD11A2.MRTWEB.A"+M+".004.LST_Day_1km.tiff",GA_Rea
dOnly)
    try:
        cols2 = band_LST.RasterXSize
        rows2 = band_LST.RasterYSize
        bands2 = band_LST.RasterCount
    except StandardError, e:
        print "Error: "+str(M)+"_LST is missing"
        exit(1)



  #  Check if LST and NDVI have the same size
    if (cols1 != cols2) or (rows1 != rows2) or (bands1 != bands2):
        print "Error: "+M+"_NDVI and "+M+"_LST have different size. Please correct
the error, delete all the output files and run the program again!"
        exit(1)
```

```
    #   Check if LST and NDVI have spatial reference
        projInfo1 = band_NDVI.GetProjection()
        transInfo1 = band_NDVI.GetGeoTransform()
        projInfo2 = band_LST.GetProjection()
        transInfo2 = band_LST.GetGeoTransform()
        if((str(projInfo1)=="") or (str(projInfo2)=="") or (str(transInfo1)=="") or
(str(transInfo2)=="")):
            print "Error: "+str(M)+" images do not spatial reference."
            exit(1)
        if((projInfo1 !=projInfo2)):
            print "Error: "+str(M)+" images have different pro spatial reference."
            exit(1)
    #   Make Matrix
        NDVI=(band_NDVI.ReadAsArray().astype(float))
        NDVI[NDVI==np.amin(NDVI)] = np.nan
        LST=(band_LST.ReadAsArray().astype(float))
        LST[LST==np.amin(LST)] = np.nan
        temp = LST
        temp = np.array(temp)
        temp.shape=(1,rows1*cols1)
        temp2 = []
        for i in temp[0]:
```

```
        if(not(np.isnan(i))):
            temp2.append(i)
    print np.amin(temp2)
    LST[LST==np.amin(temp2)] = np.nan

# Getting rid of the Nan
    i = 0
    j = 0
    v = np.ones((rows1,cols1),dtype=list)
    while i < rows1:
        while j < cols1:
            v[i,j] = (NDVI[i,j],LST[i,j])
            j = j + 1
        i = i + 1
        j = 0
    v.shape=(1, rows1*cols1)
    v=list(v)
    print type(v)
   w=[]
    i=0
    while i < rows1*cols1:
        w.append(v[0][i])
        i=i+1
```

```
        #print w[0][1]
        good = []
        for i in w:
            if ((not(np.isnan(i[0]))) and (not(np.isnan(i[1])))):
                good.append(i)
        for i in good:
            if (np.isnan(i[0]) or np.isnan(i[1])):
                print "Error!"
    #   Sort the matrix using LST and NDVI value
        sort_lst = sorted(good, key=lambda v_tuple:v_tuple[1])
        sort_ndvi = sorted(good, key=lambda v_tuple:v_tuple[0])
        print sort_lst[0]
        print len(sort_lst)
        print np.amax(sort_lst)


        NDVI_MAX_WETEDGE = sort_ndvi[-1][0]



    #   Find the NDVI value which has the highest LST
    #   In every 0.01 NDVI interval, choose 10 highest LST points and calculate the mean value
    #   Compare each highest LST and find the biggest value and its corresponding NDVI value
```

```
T_temp = []
T_start = []
i = 0
j = 0
temp1 = 0
temp2 = 0
k = 0
m = 0
ndvi_start = 0
print sort_ndvi[-1][0]
while i<sort_ndvi[-1][0]:
    while j < len(sort_ndvi):
        if i<sort_ndvi[j][0]<i+0.05:
            T_start.append(sort_ndvi[j])
        j = j + 1
    T_start = sorted(T_start, key=lambda v_tuple:v_tuple[1])
    if (len(T_start))>3:
        T_start = T_start[-3:]
    else:
        T_start = T_start[:]
    if (len(T_start)!=0):
        for p in T_start:
            T_temp.append(p)
```

```
            for o in T_temp:
                k = k + o[1]
                m = m + o[0]
            k = k / len(T_temp)
            m = m / len(T_temp)
            if temp1 >= k:
                temp1 = temp1
                temp2 = temp2
            else:
                temp1 = k
                temp2 = m
        print temp1, temp2 , len(T_temp)
        j = 0
        T_start = []
        T_temp = []
        i = i + 0.05
        k = 0
        m = 0
    ndvi_start = temp2
    print temp1
    print temp2


#   Calculate the Dry Edge
```

```
    #   In every 0.01 NDVI interval, find the highest 5 LST points. Recode them and their corresponding NDVI value
        i = ndvi_start
        j = 0
        c=[]
        z_max=[]
        z_max_temp =[]
        if (i >= sort_ndvi[-1][0]):
            return "Please check the data, something might be wrong."
        if (i<sort_ndvi[-1][0]):
            while i<sort_ndvi[-1][0]:
                while j < len(sort_lst):
                    if i<sort_ndvi[j][0]<i+0.05:
                        c.append(sort_ndvi[j])
                    j=j+1

                if len(c)==0:
                    print "c = 0"
                c=sorted(c, key=lambda v_tuple:v_tuple[1])
                print len(c)
                if len(c)>10:
                    z_max_temp = c[-10:]
                if len(c)<=10:
```

```
            z_max_temp = c[:]


        print len(z_max_temp)
        print "##############################"


        for j in z_max_temp:
            z_max.append(j)


        j=0
        c=[]
        z_max_temp =[]
        i=i+0.05
        print i
    z_max=sorted(z_max, key=lambda v_tuple:v_tuple[0])
    print len(z_max)


#   Calculate Wet Edge
  LST_min = sort_lst[0][1]
  print "**************"
  print "LST_min",LST_min


#   Ready to draw the dry edge and wet edge
  m=[]
```

```
    n=[]
    for s in z_max:
        m.append(s[0])
        n.append(s[1])

#   regression
    p = np.polyfit(m,n,1)
    print p
    p=list(p)
    print p[0],p[1]
    slope=p[0]
    #slope = -18.508
    intercp=p[1]
    #intercp = 48.537
    y=[]
    x1=range(0,200)
    x=[]
    y2=[]
    for i in x1:
        y1=float(i)*slope/100+intercp
        y.append(y1)
        x.append(float(i)/100)
        y2.append(LST_min)
```

```
    plt.plot(x,y,"r-",NDVI,LST,"r*",m,n,"b*",x,y2,"r-")
    plt.axis([0,0.9,20,55])
    plt.xlabel("NDVI")
    plt.ylabel("Temperature/c")
    plt.text(0.3,50,'LST ='+str(slope)+'*NDVI'+'+'+str(intercp))
    plt.text(0.3,52,"Date: "+M)
    plt.text(0.3,48,"Wet Edgy = "+ str(LST_min))
    savefig(str(M)+'.png')
    plt.close()
    print slope,intercp

#   write regression equation to txt
    M = str(M)
    f = open("output.txt","a")
    print >>f , "\n"+"Dry Edge Equation"
    if Count > 0:
        f.write(M+": LST="+ str(slope) + "*NDVI+" + str(intercp)+"\n")
        Count = Count - 1
    if Count == 0:
        f.close()

#   calculate TVDI
    TVDI=(LST-LST_min)/(intercp+slope*NDVI-LST_min)
```

```
    TVDI[TVDI<0]=0
    TVDI[TVDI>1]=1

#   write TVDI to disk
    M = str(M)
    driver = gdal.GetDriverByName("GTiff")
    outDataset = driver.Create(M[2:]+"_TVDI.tif",
                    cols1,rows1,bands1,GDT_Float32)
    projInfo = band_NDVI.GetProjection()
    transInfo = band_NDVI.GetGeoTransform()
    outDataset.SetProjection(projInfo)
    outDataset.SetGeoTransform(transInfo)
    TVDI_band = outDataset.GetRasterBand(1)
    TVDI_band.WriteArray(TVDI[:,:])
    TVDI_band.FlushCache()
    TVDI_band = None
    outDataset = None

#   calculate DSI
    DSI = TVDI*slope*(-1)
#   write DSI to disk
    driver = gdal.GetDriverByName("GTiff")
    outDataset = driver.Create(M[2:]+"_DSI.tif",
```

```
                    cols1,rows1,bands1,GDT_Float32)
    projInfo = band_NDVI.GetProjection()
    transInfo = band_NDVI.GetGeoTransform()
    outDataset.SetProjection(projInfo)
    outDataset.SetGeoTransform(transInfo)
    DSI_band = outDataset.GetRasterBand(1)
    DSI_band.WriteArray(DSI[:,:])
    DSI_band.FlushCache()
    DSI_band = None
    outDataset = None
#   delete variables and release memory
    del band_NDVI, cols1,rows1,bands1, band_LST, cols2, rows2,bands2
    del projInfo1,transInfo1,projInfo2,transInfo2
    del good,NDVI,LST
    del v,w,f,Count
    del sort_lst,sort_ndvi
    del T_temp,T_start
    del c,z_max,z_max_temp
    del m,n
    del p,y,x1,x,y2,slope,intercp
    del TVDI,driver,outDataset,projInfo,transInfo,TVDI_band,RSM,RSM_band
    gc.collect()
```